MODELING WATER TEMPERATURE IN SMALL AGRICULTURAL DRAINAGE

WATERCOURSES

By

Dawn Shepard

A thesis submitted in partial fulfillment of
the requirements for the degree of

MASTERS OF SCIENCE IN ENGINEERING

WASHINGTON STATE UNIVERSITY
School of Engineering and Architecture

AUGUST 2005

To the Faculty of Washington State University:

The members of the Committee appointed to examine the thesis of Dawn Shepard find it satisfactory and recommend that it be accepted.

_____
Chair

_____

_____

ACKNOWLEDGEMENTS

MODELING WATER TEMPERATURE IN AGRICULTURAL DRAINAGE

WATERCOURSES

Abstract

By Dawn Shepard, M.S.
Washington State University
August 2005

Chair: Shulin Chen

The historical practice of excavating accumulated sediment and vegetation from agricultural drainage watercourses has raised controversy between agricultural and environmental interests in King County. These low gradient channels play a critical role in draining flood waters from agricultural land and also serve as potential rearing habitat for ESA-listed salmonids. Protective policies require the application of Best Management Practices following drainage watercourse maintenance, but the effectiveness and efficiency of required practices is not well defined. Water temperature is a potentially important habitat limiting water quality parameter that may be impacted by drainage maintenance. Preferred temperatures for rearing salmonids are in the range of 12-14°C. Lethal temperature is approximately 26°C. One of the most manageable and potentially significant influences on water temperature is the shade of riparian vegetation. Riparian vegetation is typically partially cleared during drainage maintenance in order to remove accumulated sediment and reed-canarygrass. The removal of vegetation and change in channel morphology raises concern regarding the impact of drainage maintenance on watercourse temperature. Mitigation plantings are required following watercourse maintenance, yet the effectiveness of these plantings in protecting watercourse

temperature is not known. Information on the relationship between water temperature, riparian vegetation and shade is critical for developing mitigation plans.

The shade effectiveness of pre-maintenance existing vegetation versus mitigation plantings, and the impact of riparian shade on water temperature were evaluated with a reach scale study. Short reaches with uniform vegetation and uniform channel morphology were studied during summer base-flow conditions. Water temperature monitored above and below the experimental reach was used to develop and validate a physically based temperature model. Direct solar radiation was measured in and out of the shade of riparian vegetation to calibrate vegetation density for willows, Himalayan Blackberry and reed canarygrass. The developed model was found to be accurate to within 0.5 °C. Calibrated densities for buffers with complete uniform willow vegetation were 93% for mature willows, and 80% for willows approximately two years after planting. Reed canarygrass and Himalayan Blackberry growing uniformly at maturity were found to have approximately 100% calibrated densities. The difference in density between vegetation types was not found to have a significant impact on watercourse temperature. However, the presence of shade from riparian or topographic features was found to influence temperature. Narrow watercourses with vertical banks were found to be more sensitive to riparian vegetation characteristics, while wider watercourses with shallow side slopes were found to be more sensitive to air temperature. Temperature model results show that a steep incised bank increases the effectiveness of vegetation in providing riparian shade, and that shade cast by vegetation and the bank itself can decrease maximum seven day average temperatures by at least 0.7 °C.

TABLE OF CONTENTS

Page

LIST OF TABLES

LIST OF FIGURES

LIST OF VARIABLES

Channel Dimension Parameters

A_s : Segment surface area (m^2)

WWidth : Water top width (m)

b: Channel bottom width (m)

D : Water depth (m)

Beer-Lambert Law Parameters

A_{0a} : The total opaque area due to the absorbers (m^2)

A : Cross-sectional area (m^2)

I_o: the intensity entering the sample at z = 0

I_z: the intensity entering the infinitesimal slab at z

dI: the intensity absorbed in the slab

I: the intensity of light leaving the sample

σ_A : Cross-sectional area of a molecule represented as an opaque disk (m^2)

F_a : Fraction of photons absorbed

N : Number of molecules per volume

Water Characteristic Parameters

T : Water temperature °C

ρ_{water} : Density of water (kg/m^3)

$c_{p(water)}$: Heat capacity of water (cal/kg-°C)

V : Volume of water (m^3)

ΔT : Change in temperature for a single distance step during the simulation minute (°C)

c_p : Heat capacity of water (cal/kg-°C)

ε_{water} : Emissivity of water (0.95)

Time Parameters

Γ : Day Angle (radians)

JD: Day number of the year (Julian Day)

E_t : The equation of time (minutes)

L_s : Standard longitude (degrees)

L_L : Local longitude (degrees)

L_t : Time correction for longitude (minutes)

Heat Fluxes

Φ : General heat energy flux (cal/m^2-min)

Φ_{solar} : Flux due to shortwave direct and short wave diffuse solar radiation (cal/m^2-min)

$\Phi_{longwave}$: Flux due to long-wave solar radiation from the atmosphere and riparian

vegetation (cal/m^2-min)

$\Phi_{evaporation}$: Flux due to evaporative heat loss (cal/m^2-min)

$\Phi_{convection}$: Flux due convection at the air water interface (cal/m^2-min)

$\Phi_{streambed}$: Flux due to conduction between the water column and stream bed (cal/m^2-min)

Φ_{SRC} : Extra terrestrial solar constant (cal/m^2-min)

Φ_{SRE} : Flux from direct solar radiation at the earth's outer atmosphere (cal/m^2-min)

Φ_{SRA} : Flux from direct beam solar radiation routed through the atmosphere (cal/m^2-min)

Φ_{total} : Total heat flux (cal/m^2-min)

Earth Sun Physical Relationship Parameters

r : Ratio of the earth to sun distance, to average earth to sun distance (dimensionless)

$Trans_{atm}$: Transmissivity of the atmosphere (dimensionless)

θ_{sun} : Solar altitude (radians)

θ_{LAT} : Latitude (radians)

τ : Angular rotation of time (radians)

M: Optical air mass thickness (m)

Elevation: site elevation above sea level (m)

Vegetation Parameters

λ : Riparian extinction Coefficient (m^{-1})

VegDensity: Density of riparian vegetation (dimensionless)

$VegH_{actual}$: Height of riparian vegetation (m)

Veg_{width} : Width of vegetation from bankfull edge perpendicular to the bank (m)

PL_{veg} : Approximated path length of solar radiation through riparian vegetation (m)

$Transverse_0$: Distance from the water's edge to the bankfull mark (m)

Bed Conduction Parameters

σ : Stefan-Boltzmann constant (1.83 x 10^{-11} cal/cm^2-min)

ρ_{bed} : Volumetric weighted density (kg/m^3)

$\rho_{seidment}$: Substrate density 1600 (kg/m^3)

α_{water} : Water volume ratio (dimensionless)

$\alpha_{sediment}$: Sediment volume ratio (dimensionless)

$D_{sediment}$: Depth of conduction layer (m)

K_{water} : Water thermal conductivity 0.60 (J/ m s °C)

$K_{sediment}$: Sediment thermal conductivity 15.98 (J/ m s °C)

K_{bed} : Volumetric composite thermal conductivity in conduction layer (J/ m s °C)

v_{water} : Water volume in conduction layer (m^3)

$v_{sediment}$: Substrate volume in conduction layer (m^3)

$v_{Hyporeic}$: Total volume in conduction layer (m^3)

$\vartheta_{sediment}$: Porosity of the conduction layer (dimensionless)

$\Psi_{sediment}$: Substrate thermal diffusivity (m^2/s)

Ψ_{water} : Water thermal diffusivity (m^2/s)

CHAPTER 1
INTRODUCTION

Water temperature is critical to the chemical and biological processes that define

the health of aquatic environments (Brown 1967, USEPA 1997). Elevated temperatures

negatively affect salmonid growth rate, metabolism, and disease resistance, as well as the

timing of adult migrations, fry emergence and smoltification (NOAA 2004). Temperature

limits the maximum concentration of oxygen that can remain dissolved in water and

available to aquatic organisms. Water temperature has been identified as an important

factor limiting salmonid rearing habitat and contributing to the decline in salmon

population in streams throughout the Pacific Northwest including in the Puget Lowlands

(**http://www.salmonrecovery.gov/strategy.shtml**).

Chinook salmon prefer water temperatures between 12 and 14°C with

approximately 50% mortality occurring at 26.2 °C (Meehan 1991). Current EPA

guidelines for Class A waters require a single daily maximum temperature not more than

18°C. Most lowland waters that support salmonid rearing, spawning, and migration will

be designated under Class A protection. Few water bodies will be designated under Class

B protection, which requires a single daily maximum of not more than 21°C and is aimed

at protecting salmonid rearing and migration but not necessarily spawning (EPA 2002).

Water quality standards are undergoing revision after EPA's review of field and

laboratory studies of chronic sub-lethal and lethal temperature effects on fish (EPA

2002). A small, single daily fluctuation beyond a defined daily maximum temperature

was found not to be biologically meaningful (EPA 2002). A metric that is overly

averaged, such as the seven day average of daily mean temperatures, could mask

regularly occurring large diurnal temperature variations out of healthy range (EPA 2002).

The seven day average of daily maximum temperatures is the metric identified as the

most useful in providing full protection for the individual life-history stages of key

species (EPA 2002). For salmon and trout migration and non-core juvenile rearing in the

lower part of river basins the proposed seven day average of daily maximum temperature

is 18 °C (EPA 2002).

Bormann (2000) lists 45 environmental and physical factors influencing stream

water temperature. Among these factors are weather conditions such as air temperature,

relative humidity, and wind speed, stream site physical characteristics such as stream

width, depth and roughness, and the presence of shading vegetation and topography

(Brown 1967, Beschta 1984, Bartholow 1991, Brown 1987, and Edinger 1968).

Controversy exists regarding the relative importance of riparian vegetation in moderating

stream temperatures. It has been argued that solar radiation is the dominant factor

influencing stream temperatures and that the shade of riparian vegetation can

significantly reduce stream warming (Brown 1969, Beschta 1997, Theurer 1985, and

Chen 1997). Despite a large number of studies there is no consensus on the importance of

shade in determining water temperature. Some believe air temperature is primarily

responsible for driving stream temperatures and that solar radiation and riparian shade are

not significant (Larson and Larson 1997, Larson and Larson 1996, Sullivan et al. 1990,

Zwieniecki and Newton 1999). Unlike the influence of ambient weather conditions,

riparian vegetation and channel dimensions are uniquely manageable watercourse

characteristics. If these characteristics are important to stream temperature, their influence should be determined to identify and prevent anthropogenic temperature increase.

Low gradient agricultural watercourses in King County serve as rearing habitat for ESA-listed salmonids and play a critical role in draining flood waters from agricultural lands. To facilitate drainage, these watercourses have been routinely excavated to remove accumulated sediment and watercourse vegetation. Riparian vegetation is typically partially or completely removed on one bank in the course of drainage watercourse maintenance. Mitigation practices are prescribed in association with maintenance in an effort to repair any environmental damage caused by maintenance. The effectiveness of currently required mitigation plantings, and the vegetation type and minimum planting density necessary to protect water temperature are not known. The objective of this study is to identify the impacts of maintenance and mitigation on water temperature.

In addition to protecting water from solar exposure and warming, riparian buffers can serve a variety of functions such as reducing bank sediment erosion, providing plant and animal habitat, and providing a source of woody debris. On agricultural lands in King County, riparian areas have been extensively modified over many years and invasive reed canarygrass is dominant in many locations, although sections of some watercourses still maintain up to 90% native vegetation (U.S. Army Corps Of Engineers, 1997). This study does not address the function of those areas that still maintain up to 90% native

vegetation, or the impact of maintenance and mitigation in those areas. Instead, this study focuses on the dominant reed canarygrass and Himalayan Blackberry vegetation. An understanding of minimum mitigation required to replace the shade benefits of these plants after maintenance will make maintenance and mitigation more economical, and preserve agricultural land.

Goals and Objectives

The goal of this project is to determine the impact of maintenance on the temperature of small agricultural watercourses by identifying the temperature influence of maintenance design characteristics such as riparian vegetation, channel width, and channel side slope. Specific tasks required to accomplish this goal include:

- Identify the impact of watercourse shade on water temperature
- Identify the effectiveness of Sitka willows, Himalayan Blackberry and reed canarygrass riparian vegetation in providing watercourse shade
- Develop and customize a modeling tool to determine the water temperature impact of maintenance plan scenarios
- Model diurnal temperature on an hourly basis to identify changes in water temperature due to design characteristics, producing simulated data also suitable for use in nutrient and dissolved oxygen modeling efforts
- Field data collection to support model development, calibration and verification.

The focus of this study is to identify minimum, cost efficient mitigation for watercourse maintenance. Consistent with the intended purpose, this study focuses on identifying the shade benefits provided by existing vegetation versus vegetation typically planted for mitigation purposes. Vegetation types that commonly exist along small agricultural watercourses in King County prior to watercourse maintenance include reed canarygrass (*Phalaris arundinacea)* (RCG) and Himalayan Blackberry *(Rubus discolor)*. Willows such as Sitka willow (*Salix Sitchensis*) are commonly planted as part of mitigation that follows maintenance. This study focuses on thermal impacts because temperature is the fundamental water quality parameter and can significantly determine a water body's suitability for supporting aquatic life. Because water temperature influences all other water quality parameters, another critical function of water quality modeling is to support modeling efforts for other parameters such as dissolved oxygen.

CHAPTER 2
LITERATURE REVIEW

Contemporary stream temperature models rely on physically based energy balance and mass transport equations to mathematically describe the processes that drive system behavior. Empirical models are equations that relate a selected number of measured input parameters, such as ambient air temperature, to an observed response, such as water temperature. The components of empirical models may not have a direct meaning in physical reality. Empirical models are not necessarily applicable to locations or systems other than the one for which they were developed while models based on the laws of physics are true everywhere. Empirical models are appropriate when the physical mechanisms that determine system response are not known. While no temperature model is entirely physically based, entirely empirical temperature models are not well suited to identify the impact of changes in individual physical watercourse characteristics such as channel width, depth, or the distance from the watercourse to shading vegetation on its bank.

Bormann (2000) lists 45 environmental and physical factors influencing stream temperatures. Among these factors are weather conditions such as air temperature, relative humidity and wind speed, stream site physical characteristics such as stream width, depth and roughness, and the presence of shading vegetation and topography. Brown (1967) initially identified the importance of forest cover in protecting stream temperature caused by an increase in the stream's exposure to solar radiation. He

compared water temperature at the outlet of forested and harvested watersheds over two years and found that clearcutting increased the daily change in temperature by 14 degrees Fahrenheit in the month of August. Brown (1969) applied the heat energy balance method to small streams and pointed out the utility of temperature modeling in managing stream temperature. Brown (1967) pointed out that because small streams carry smaller volumes of water, the temperature of small streams is more responsive to net energy exchange than larger rivers and therefore more accuracy is required of an energy balance model to achieve a given accuracy in temperature prediction.

Energy balance methods account for predicted incoming and outgoing heat fluxes to result in an estimate of the net flux of energy received by a segment of water in a stream. The following equation is a general energy balance equation similar to the one used by Brown (1969):

$$\Phi_{total} = \Phi_{solar} + \Phi_{longwave} + \Phi_{evaporation} + \Phi_{convection} + \Phi_{streambed} \qquad \textbf{2.1}$$

where Φ_{solar} is the sum of shortwave direct and short wave diffuse solar radiation penetrating the stream's surface, $\Phi_{longwave}$ is the sum of long-wave solar radiation reaching the water's surface through the canopy opening and streamside vegetation, $\Phi_{evaporation}$ is the flux representing heat loss due to evaporation, $\Phi_{convection}$ is the heat flux due convection at the air water interface, and $\Phi_{streambed}$ is the flux experienced due to conduction between the water column and stream bed.

The range of magnitudes of the heat flux terms described, have been outlined by McCutcheon (1999). According to McCutcheon, short wave solar radiation ranges from approximately 50 to 500 W/m^2, long wave atmospheric radiation ranges from approximately 30 to 450 W/m^2, long wave radiation emitted from a water body ranges from approximately 300 to 500 W/m^2, evaporative heat loss ranges approximately 100 to 600 W/m^2, convective heat exchange ranges approximately 100 to 600 W/m^2.

The change in stored energy determined by the balance of these fluxes is converted to a change in stream temperature. The amount of heat transferred by a flux is equal to the heat flux times the receiving area:

$$\Delta H = \Phi \cdot A \qquad\qquad \textbf{2.2}$$

where ΔH is the heat energy transferred (calories/min), Φ is the heat energy flux (cal/m^2-min), and A is the receiving area (m^2). A general equation for the change in water temperature due to heat exchange with the environment is as follows (McCutcheon 1999)[1]:

$$\frac{\partial T}{\partial t} = \frac{\Phi_{total} \cdot A_s}{\rho_{water} \cdot c_{p(water)} \cdot V} \qquad\qquad \textbf{2.3}$$

---

[1] Although the bed conduction flux included in the term Φ_{total} is not associated with the water surface area directly, for rectangular channels, the surface area of a stream segment is equal to the area of the channel bottom.

where T is the water temperature (°C), ρ_{water} is the density of water (kg/m³), $c_{p(water)}$ is the heat capacity of water (cal/kg-°C), V is the volume of water (m³), A_s is the stream surface area (m²), and Φ_{total} is the total heat flux (cal/m²-min).

Brown attained temperature predictions within ±1°F with his energy balance method using site specific measured meteorological and solar radiation data (1969). He noted the importance of onsite meteorological data and the error introduced using data that does not accurately represent solar radiation reaching the water's surface due to shade from riparian vegetation. Brown's application of the energy balance to small streams was followed by the development of several more detailed models using equations to predict solar radiation at the earth's surface. With the use of these equations less site specific solar radiation data is required to accurately model water temperature (McCutcheon 1999). In 1972, Wunderlich presented an equation to calculate the short-wave solar flux reaching the earth's outer atmosphere as a function of solar altitude:

$$\Phi_{SRE} = \frac{\Phi_{SRC}}{r^2} \sin\theta_{sun} \qquad\qquad 2.4$$

where Φ_{SRC} is the extra terrestrial solar constant (cal/m²-min), Φ_{SRE} is the direct solar radiation received at the earth's outer atmosphere (cal/m²-min), θ_{sun} is equal to the solar altitude (radians), and r is the ratio of the earth to sun distance to the average earth to sun distance (dimensionless) as given by:

$$r = 1 + 0.017 \cdot \cos\left(\frac{2\pi}{365}(186 - TJ)\right) \qquad\qquad 2.5$$

where TJ is the Julian day plus day fraction.

       To predict the solar flux at the earth's surface, the attenuation and scattering of radiation in the earth's atmosphere must be accounted for. Ibqal (1983) describes short-wave solar radiation reaching the earth's surface as:

$$\Phi_{SRA} = \Phi_{SRE} \cdot Trans_{atm}^{M} \cdot \cos\theta_{zenith} \qquad\qquad 2.6$$

where Φ_{SRA} is the direct beam solar radiation routed through the atmosphere (cal/m^2), $Trans_{atm}$ is the transmissivity of the atmosphere (dimensionless), M is the optical airmass thickness (meters), and θ_{zenith} is equal to the solar zenith angle (radians).

The transmissivity of the atmosphere is described by:

$$Trans_{atm} = 0.0685 \cdot Cos\left(\frac{2 \cdot \pi}{365} \cdot (JD + 10)\right) + 0.8 \qquad\qquad \mathbf{2.7}$$

In equation 2.6 the optical air mass thickness can be calculated as a function of the observer's elevation and the altitude of the sun as reported by Beschta (1984).

$$M = \left[\frac{\left(\dfrac{288 - 0.0065 \cdot elevation}{288} \right)^{5.256}}{\sin \theta_{sun} + 0.15 \cdot \left(\dfrac{180 \cdot \theta_{sun}}{\pi} + 3.855 \right)^{-1.253}} \right]$$

<div align="right">**2.8**</div>

where elevation refers to the site elevation above sea level (meters). Following this general description of the energy and mass balance approach, is a more specific description of several commonly used stream temperature models.

Stream Temperature Model: TEMP86

The model TEMP86, by Beschta and Wethered (1984), is a physically based model that predicts solar radiation at the earth's surface and estimates the interception of solar radiation by riparian vegetation. Beschta describes the attenuation of solar radiation in the vegetation buffer using vegetation transmissivity. Like atmospheric transmissivity, vegetation transmissivity determines how effectively vegetation attenuates and scatters radiation before it can reach the water's surface. The equation is written as:

$$\Phi_{SolarVeg} = \Phi_{SRA} \cdot Transmissivity_{Veg}{}^{PathLength}$$

where *PathLength* equals the distance radiation travels through vegetation before reaching the water's surface. A vegetation coefficient is used to calculate vegetation transmissivity as follows (Beschta 1984):

$$Transmissivity_{Veg} = 1 - 0.9 \cdot Vegetation_{coefficient} \qquad \textbf{2.9}$$

where $Vegetation_{coefficient}$ is the vegetation coefficient representative of the buffer volume

responsible for attenuation and scattering of radiation. The vegetation coefficient

described by Beschta is not readily measured in the field for application in temperature

models (http://www.deq.state.or.us/wq/HeatSource/HeatSource.htm).

Stream Temperature Model: HSPF and the Model SHADE

An alternative method to describe attenuation of solar radiation by vegetation was

developed by Chen (1993) with the model SHADE. Chen et al. made an extensive

comparison of stream temperature models (1993) and evaluation of their predictive

capabilities to determine that none had full capabilities to dynamically simulate

temperature on a watershed scale. As a result, Chen *et al*. developed a watershed scale

stream temperature model including a stand-alone program called SHADE to

dynamically adjust solar radiation data for water temperature simulation within the model

Hydrologic Simulation Program-Fortran (HSPF) based on vegetation and topographic

shading characteristics. The shade model assumes that for vegetation near the stream's

edge, vegetation will overhang the water by ten percent of its width. The error introduced

by this assumption will be largest in the case of uniform vegetation with extensive or

minimal overhang existing close to a small watercourse.

Chen applied the Beer-Lambert law to describe the extinction of solar radiation as

it passes through riparian vegetation based on vegetation density. Chen's method replaces

the one used by Beschta. Instead of a vegetation coefficient, Chen's model requires

vegetation density as an input, which can be observed in the field or with the use of

stream aerial photographs. Chen's model is described as follows:

$$Shade_{Density} = 1 - \exp(-\lambda \cdot PathLength) \qquad \textbf{2.10}$$

where $Shade_{Density}$ is the density of shadow cast by vegetation and

$$\lambda = -\frac{Ln(1 - VegDensity)}{VegH_{actual}} \qquad \textbf{2.11}$$

To determine the amount of solar radiation reaching the water's surface, the length of a

shadow cast on the water's surface is multiplied by its density to result in an effective

shade length.

$$Shadow_{Length} = Shadow \cdot Shade_{Density} \qquad \textbf{2.12}$$

where $Shadow$ is the actual shadow length and $Shadow_{Length}$ is the effective shadow

length. Solar radiation received by the water's surface is then calculated as:

$$\Phi_{Veg} = \Phi_{SRA} \cdot \left(1 - \frac{Shadow_{Length}}{WWidth}\right) \qquad \textbf{2.13}$$

Chen et al. (1997) successfully applied HSPF and the model SHADE in

watershed scale modeling efforts. Stream temperature modeling on the Grande Ronde

watershed was performed to provide guidance for riparian restoration activities (Chen et

13

al. 1997). The SHADE model used topographical shade angles, and riparian vegetation dimension and location information to adjust global solar radiation reaching the stream's surface. HYDR The hydraulic module of HSPF, calculated wetted width on an hourly basis. Stream bed conduction, although acknowledged to be a potentially important factor for smaller watercourses was neglected. Among Chen's conclusions were that natural weather cycles could not moderate stream temperature for the survival of salmon. Riparian vegetation is noted as the only critical manageable factor to significantly reduce lethal and sub-lethal temperatures. It was noted that wider reaches could not be sufficiently shaded to reach target standards of maximum summer temperature 16°C and seven day average maximum of 14.5°C. Model predictions showed that 41 out of 51 reaches could reach target standards with restored buffers. Model accuracy was 2.8 to 3.0°C (Chen et al. 1997).

Stream Temperature Model: Heat Source

Much of the methodology for modeling solar radiation above and below a riparian buffer used in TEMP86, as well as the riparian extinction coefficient proposed by Chen (1993) in the model SHADE, were later applied in the development of the model Heat Source. The first model Heat Source was a simple reach scale model, using the methods described by Beschta to account for the shade of riparian vegetation. Heat Source 6 applies Chen's model SHADE. Version 6 accepts dynamic weather and tributary temperature data but constant flow rates. Heat Source has since evolved into a watershed scale model (v. 7.0) capable of accepting data that represent great spatial detail in channel morphology and riparian vegetation as well as dynamic weather and stream flow data.

14

One of the most significant challenges in applying this model is providing input data with the spatial extent and accuracy that the model can effectively utilize (http://www.heatsource.info). HSPF and Heat Source 7.0 are detailed models suited to temperature predictions on a watershed scale and are less suited to the small watercourses of interest in this study.

Stream Temperature Model: SSTEMP

The Stream Segment Temperature Model (SSTEMP) is the reach scale version of SNTEMP, a steady state average daily model that uses physical relationships and vegetation density to predict solar radiation reaching the water's surface. Like many stream temperature models, it is hydraulically strictly steady state and does not attempt to consider changes in temperature by depth or location across a stream cross-section. Change in temperature is modeled only in the downstream direction. Because it is an average daily model, the shortest possible time period for averaging is 24 hours. All inputs are in the form of daily to yearly mean values, and are applied uniformly over a reach. SNTEMP does not accept changing hydrological or meteorological data provided on a regular time step, and thus performs poorly where dynamic or diurnal behavior is of interest. This makes SNTEMP less suited to handle diurnal temperature changes and is an important limitation of the model (Bartholow 2000).

Daily maximum temperature (or afternoon average stream) is often of interest in the study of thermal pollution or temperature as a habitat-limiting factor. Because of the importance of ambient air temperature and weather conditions in determining stream

temperature, SNTEMP approximates a maximum ambient temperature using an empirical equation to simulate fluctuations around the average daily input value. Since this empirical equation was developed and calibrated in one watershed, it is not necessarily suited to all locations and should be calibrated or re-developed based on local conditions. This approach to calculating daily maximum or afternoon average temperature is likely to be a source of error despite calibration. SNTEMP also makes the assumption that the fluctuation in temperature from daily average to daily maximum is equal in value to the change in temperature between daily average and daily low temperature. In general SNTEMP gives thorough treatment of each possible source and sink of heat including the influence of shade from topography and vegetation. The primary sources of error in SNTEMP are daily averaging and the model's inability to accept meteorological data (Bartholow 2000).

Stream Temperature Model: QUAL2E

The USEPA model QUAL2E has been used extensively and contains a basic hydrologic model. QUAL2E performs a quasi-dynamic analysis by accepting dynamic meteorological inputs with steady-state flow values. The model has the capability to accept changing meteorological data taken at a regular time interval, and to behave quasi dynamically for diurnal temperature simulation. QUAL2E also has the ability to produce steady-state results if dynamic meteorological data is not available. In older versions of this software, meteorological information was applied equally to all locations in the watershed, but newer versions allow this data to vary spatially. Although QUAL2E can accept dynamic forcing functions such as ambient temperature and other meteorological

16

factors, the hydrologic forcing functions must be constant. All flows and boundary conditions are constant for the QUAL2E model, as they are in SNTEMP. QUAL2E, despite its advanced quasi-dynamic capabilities, is lacking in consideration of factors shown to be potentially significant in modeling stream temperature. QUAL2E does not model riparian vegetation shading and neglects bed conduction (Brown 1987).

Environmental Factors Driving Stream Temperature

Despite a large number of stream temperature studies, controversy exists regarding the effect of shade and riparian vegetation on water temperature. Larson and Larson (1997) suggest that the rate of stream temperature change can be attributed to the gradient in temperature between air and water, on the basis that air temperature is an indicator of the thermal environment. They point out that difference in air temperature from high to low elevations is significantly due to the cooling of air as it expands at higher elevations where it is exposed to lower atmospheric pressure. Larson and Larson (1997) point out that flow velocity determines how long water is exposed to a particular thermal environment. They attribute changes in stream temperature as water flows from high to low elevations to the corresponding change in air temperature to which the stream is exposed. Larson and Larson do not mention solar radiation and shade as an additional significant factor in stream heating. They observe that at a minimum, flow velocity as well as air and water temperature above and below a reach of interest, should be measured in order to draw any conclusions about the influence of the environment on water temperature.

In a very simple experiment by Moore et al. (1999), equal water volumes with similar initial temperatures were placed into tanks insulated on the sides and bottom. One tank was exposed to August solar radiation and one was completely shaded by tarps. Results showed that the shaded tank was significantly cooler over the course of the study, though the tanks were exposed to the same ambient temperatures. A similar study was conducted using running water with similar results, demonstrating the potential importance of solar radiation and shade in determining water temperature (Petersen et al 1999). This simple experiment affirms the importance of consideration for stream shade in modeling efforts such those of Beschta, Chen and others. The work of Beschta and Chen does not appear to deny the importance of air temperature as one influence on water temperature, but include additional consideration for the streams solar radiation exposure or sheltering.

Review of the Selected Water Temperature Model: Heat Source

Heat Source 6 was selected for adaptation and application in this reach scale study to identify the importance of riparian vegetation because of its treatment of riparian vegetation and meteorological conditions as well as its adaptability and ease of use. Heat Source 6 is a program written in Visual Basic for Applications in Excel. Heat Source 6 includes the critical considerations of shading from topographical features and riparian vegetation. It simulates water temperature on an hourly basis, accepting weather data records on an hourly basis. Heat Source 6 is suited for diurnal temperature prediction to support dissolved oxygen modeling and is readily adaptable for use as a reach scale model. The model accepts detailed information describing the dimensions and density of

riparian vegetation, including the vegetation's measured overhang length. Heat Source 6 is a widely available share-ware program. Because it is written in Visual Basic for Excel, the model does not require management or formatting of external data files to supply required data such as hourly weather data. Weather and other input data may be formatted and stored directly in the designated worksheet locations in the Heat Source Model. This system is convenient since the input data used in simulation is stored with results and can be easily altered for the next scenario. Heat Source version 6 was selected for use as the base model in this study to determine the impact of changes to channel characteristics and riparian vegetation associated with excavation for watercourse maintenance and mitigation plantings. Heat Source 6 was designed as a daily model, accepting one day's continuous data and reporting one day's simulation results, although the simulation may be repeated over several days, only the last day is stored and reported.

The riparian extinction method applied by Chen *et al*. in the model SHADE is used to simulate shade in Heat Source 6. As presented at **http://www.chem.vt.edu/chem-ed/spec/beerslaw.html,** the Beer-Lambert Law can be derived by approximating molecules in solution as opaque disks whose cross-sectional area σ_A, represents the effective area seen by a photon of frequency *w*. Figure 2.1 represents an infinitesimal slab, dz, of sample:

Figure 2.1 Conceptual differential volume used to illustrate the Beer-Lambert law
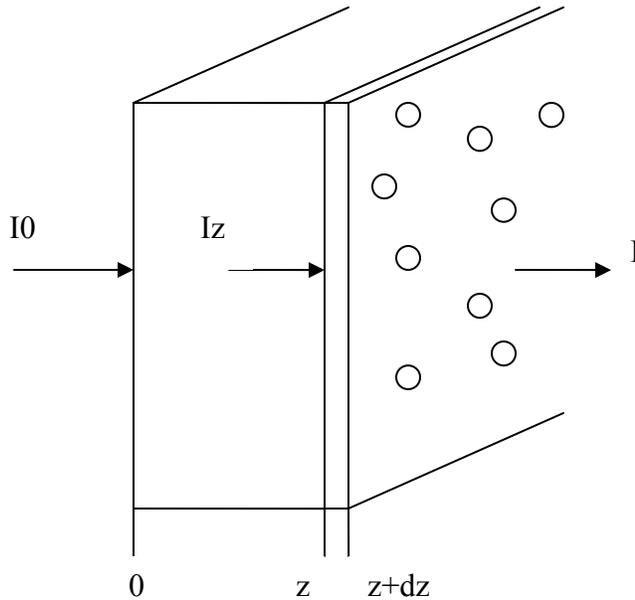
$$A_{0a} = \sigma_A \cdot N \cdot A \cdot dz \qquad\qquad\qquad\qquad \textbf{2.14}$$

where A_{0a} is the total opaque area on the slab due to the absorbers, A is the sample cross-sectional area, I_o is the light intensity entering the sample at $z = 0$, I_z is the light intensity entering the infinitesimal slab at z, dI is the light intensity absorbed in the slab, I is the light intensity of light leaving the sample, σ_A is the cross-sectional area of a molecule represented as an opaque disk, and N is the number of molecules per volume.

The fraction of photons absorbed is represented as the fraction of absorbing area to total area as:

$$F_a = \frac{\sigma_A \cdot N \cdot A \cdot dz}{A} \qquad\qquad\qquad\qquad \textbf{2.15}$$

where F_a is the fraction of photons absorbed.

The ratio of light intensity entering the slab to that leaving the slab is proportional to the fraction of photons absorbed.

$$\frac{dI}{I_z} = -\sigma_A \cdot N \cdot dz \qquad\qquad \textbf{2.16}$$

Integrating from z = 0 to z = b gives:

$$\ln(I) - \ln(I_0) = -\sigma_A \cdot N \cdot b \qquad\qquad \textbf{2.17}$$

or

$$-\ln\left(\frac{I}{I_0}\right) = -\sigma_A \cdot N \cdot b \qquad\qquad \textbf{2.18}$$

Comparing this equation and with that from Chen et al.:

$$ShadeDensity = 1 - \exp(-\lambda \cdot PathLength) = 1 - Trans = 1 - \frac{I}{I_0} \qquad\qquad \textbf{2.19}$$

where *Trans* is the transmissivity.

Applying this model to riparian vegetation, the element through which light passes, is the riparian buffer strip with length (dx) and height equal to the vegetation buffer height. In Beer's Law above, N is the number of molecules per cubic centimeter and sigma represents the area of a molecule. When combined, these terms represent shaded area per cubic centimeter. In the infinitesimal volume, the total area shaded is the

amount of area shaded per cubic centimeter, times the infinitesimal volume size, which is A dz. The fraction of photons absorbed is the ratio of this shaded area to the total area.

In the Beer's Law model, the term $\sigma_A \cdot N$ is represented by the density of vegetation within the riparian buffer. This use of Beer's Law assumes that each vegetation object within the buffer is opaque. When vegetation density is observed for a modeled distance dx, aerial photographs are commonly used to identify the percentage of riparian buffer land area covered by vegetation for the distance dx. Because vegetation, such as a single tree or willow is not opaque, when complete land cover is achieved by vegetation, the vegetation density is the density of the vegetation type. Buffers selected for this study completely occupy the riparian zone, implying a density of 100%, with constant buffer widths, yet shadows of varying densities are cast by different vegetation types due to differences in opaqueness.

In practice, aerial photographs are often used to estimate vegetation density based on the spatial density of vegetation objects observed in the riparian zone. This density is adjusted to account for vegetation that is not opaque using a class system by vegetation type. For example, conifers may occupy the riparian zone at approximately an 80% density and confers as a class might be assumed to have 90% density. Solar Pathfinder measurements are used in the field to validate model predicted Effective Shade based on vegetation input data collected as described. Effective shade is determined by the model as follows:

$$E_{shade} = \frac{\Phi_{atmospheric} - \Phi_{vegetation}}{\Phi_{atmospheric}} \qquad \qquad \textbf{2.20}$$

If used according to the user's manual, the Solar Pathfinder does not account for plant density during field measurement of summer month effective shade. The shade of vegetation is treated the same as shade cast by buildings or solid structures. Any adjustment to account for 'lacey' shadows is at the discretion of the user. Solar Pathfinder measurements are typically made at the center of the watercourse at water level to account for bank topography. Vegetation typically has a great deal spatial variation. The point location of effective shade measurement in the field using a Solar Pathfinder is unlikely to represent the segment averaged vegetation input data developed using the plant density and class system described. By comparison, spatial variation will be a greater source of discrepancy between Solar Pathfinder measured effective shade and modeled effective shade, than imperfect estimation of vegetation density. Using a large number of measurements over a large spatial scale, Solar Pathfinder measurements have been shown to correlate will with predicted effective shade. When spatial variation is minimized or eliminated, as it is in a small uniform continuous reach of vegetation, the majority of error in effective shade estimation will be the result of neglecting to account for 'lacey' or incomplete shadow casting.

In accordance with Equation 2.1, Heat Source describes the rate of temperature change in an element of stream water as the sum of the rate change in temperature due to advection, dispersion and heat energy flux. Heat Source 6 methodology estimates the amount of energy exchanged between an element of water and its surrounding as a

23

function of air temperature, channel bed characteristics, and radiation dependent on the time of day, time of year, the location of the element of interest on the earth and its orientation to the sun (Boyd 1996).

Recall equation 2.6

$$\Phi_{total} = \Phi_{evaporation} + \Phi_{convection} + \Phi_{streambed} + \Phi_{solar} + \Phi_{longwave}$$

The evaporative heat flux represents a loss of heat from the water column. The heat loss associated with evaporation is directly related to the latent heat of vaporization (LHV) of water. The rate of evaporation from the water column is determined according to an empirical relationship developed based on studies of evaporation from open channels. The rate of evaporation is a function of the vapor pressure deficit and wind speed and can vary according to many factors including wind sheltering by riparian vegetation.

Convective heat exchange is molecular heat exchange between water and air. Convective heat exchange is a function of the same parameters that influence evaporative heat loss and is a function of an empirical ratio and the rate of evaporation. Stream bed conduction represents heat exchange between the water column and bed material. Bed conduction is a function of the equilibrium soil temperature, the depth over which the soil reaches equilibrium temperature and soil particle size. Solar radiation represented by the term Φ_{solar} , is determined through sequential steps to determine the value of solar radiation flux at four locations along its path from the sun to the water column. Direct

short-wave solar radiation is considered to radiate from the sun as a point source. The first step is calculation of solar radiation at the earth's outer atmosphere. This value is referred to as extra-terrestrial solar radiation. This approximation is based on measured values of solar radiation and a trigonometric relationship between the sun and a plane tangential to the earth (Wunderlich 1972). The second step is calculation of solar radiation reaching the outer limits of riparian vegetation. This value is a function of atmospheric transmittance. The third step is calculation of solar radiation reaching the stream's surface, accounting for shading by riparian vegetation. Finally a fraction of the solar radiation reaching the water's surface will be reflected from the water's surface as a function of the angle of incidence.

A second component of total solar radiation is short wave diffuse solar radiation. When direct short wave solar radiation reaches the earth's outer atmosphere, a fraction will be reflected and redirected so that it is no longer considered as a point source but radiates from all directions. Shortwave diffuse solar radiation reaching the outer limits of riparian vegetation is estimated as an empirical function of extra terrestrial solar radiation. The methodology presented is similar to that reported by Beschta (1984). A fraction of the available diffuse solar radiation will reach the water's surface through the opening in riparian vegetation. The remainder is considered to be blocked by vegetation. The total solar radiation reaching the water column is the sum of diffuse and direct short wave solar radiation that passes the water's surface.

Long-wave, or thermal radiation, has a positive and negative component. Long-wave radiation is emitted by both the earth's atmosphere and the water column. Long-wave radiation emitted by the water column represents the negative component, while long-wave radiation emitted by the atmosphere and received by the water column constitutes the positive component. Like diffuse solar radiation, long-wave radiation is considered to radiate from all directions.

Recall that each of the last three energy balance components discussed, direct shortwave solar radiation, short wave diffuse solar radiation, and long wave radiation, have a unique interaction with riparian vegetation. These energy balance terms are will now be described in more detail as they are calculated in Heat Source 6.0.

Short Wave Solar Radiation

As solar altitude changes over the course of the day, solar radiation may be intercepted by distant topographic features before reaching the outer limits of the riparian buffer. Interception by distant topography is accounted for in Heat Source 6 by affecting local time of sunrise or sunset. After the sun has risen over topographic features solar radiation may be intercepted by stream bank vegetation, or the stream bank itself if the stream's surface elevation is lower than the top of the bank. The vertical distance from the stream's surface to the top of the bank, must be measured in the field. For any shading feature, an angle can be calculated between the level of the water's surface and the top of the shading feature. This angle is a function of the height of the object and its distance from the mid-point of the water's surface. The model determines that a shadow

is being cast by the bank or vegetation by comparison of vegetation and topographic

angles with solar altitude. The length of a shadow is calculated based on the geometry of

riparian vegetation and the sun's position. This length is referred to as the shadow width,

and is assumed to be cast only by vegetation on the sunward bank.

The riparian area is described by the type and dimensions of vegetation in user

defined zones. Zones are consecutive strips of vegetation with a user defined width,

running parallel to the water's edge. Zone 0 is the watercourse bank itself. Zone 0 is the

zone between the water's edge and the edge of riparian vegetation. For the purposes of

this study, bankfull is synonymous with the top of the bank. Bankfull width must be

identified in the field as the point where there is a brake in slope between the sides of the

watercourse banks and relatively level floodplain. The transverse distance from the

water's edge to the bankfull mark is calculated as follows:

$$Transverse_0 = \frac{Bankfull_{Width} - Wetted_{Width}}{2}$$

2.21

where $Transverse_0$ is the distance from the water's edge to the bankfull mark (meters).

The length of shadow cast by the sunward bank itself is first approximated:

$$Shadow_{widthBank} = \frac{Incision \cdot \sin\left|\theta_{azimuth} - \theta_{aspect}\right|}{\tan\theta_{sun}}$$

2.22

The length of shadow cast by the stream bank that exists only on the water's surface is equal to this shadow length minus the transverse distance. If the shadow length minus the transverse distance is still greater than the wetted width, the fraction of the water's surface covered by the bank's shadow is set to 1. Zone 1 is the first riparian vegetation zone. Vegetation is assumed to exist at the top of the bank at the bankfull elevation. Riparian vegetation may exist between banks, but this component of vegetation is considered overhanging. Overhanging vegetation has some length that it extends beyond the edge of the top of the bank. In order to predict shadow length and the amount of the water's surface shaded by vegetation, the transverse distance from the water's edge to the leading edge of riparian vegetation is calculated as follows:

$$Transverse_1 = Transverse_0 - Veg_{Overhang} \qquad\qquad \textbf{2.23}$$

If $Veg_{Overhang}$ is greater than $Transverse_0$, a negative number would result. The transverse distance from the water's edge to the leading edge of vegetation, $Transverse_1$ is instead set to zero. This describes vegetation that begins at the water's edge.

Using a program loop, the shadow length cast by vegetation in each zone on the sunward bank, is calculated using:

$$Shadow_{width} = \frac{VegH_{apparent} \cdot \sin\left|\theta_{azimuth} - \theta_{aspect}\right|}{\tan\theta_{sun}} - transverse(zone) \qquad\qquad \textbf{2.24}$$

where *transverse*(*zone*) is the transverse distance for the particular zone.

The shade density of a shadow cast by riparian vegetation is calculated by first estimating a riparian extinction coefficient for the vegetated zone according to the methodology described by Chen et al (1998).

The length of this shadow over the water's surface is determined for each zone as the shadow length minus the transverse distance from the water's edge to the leading edge of that zone. The density of each shadow cast by vegetation is a function of the density of vegetation and the path length through vegetation as described by Chen (1998).

$$\lambda = -\frac{Ln(1 - VegDensity)}{VegH_{actual}} \qquad\qquad \textbf{2.25}$$

where λ is the riparian extinction coefficient (m^{-1}), VegDensity is the vegetation density typically estimated from aerial photographs as the percentage of land in the riparian zone occupied by vegetation (dimensionless), and $VegH_{actual}$ is the height of riparian vegetation (meters).

A uniform vegetated zone width, and therefore a path length at any point in time, is assumed for a single differential distance using:

$$PL_{veg} = \frac{Veg_{width} + Veg_{overhang}}{\left|\sin\left|\theta_{azimuth} - \theta_{aspect}\right|\right| \cdot \cos\theta_{sun}}$$ **2.26**

where Veg_{width} is the width of vegetation from bankfull edge perpendicular to the bank

(meters) and PL_{veg} is the approximated path length of solar radiation through riparian

vegetation (meters).

The fraction of the water's surface shaded by the bank receives no solar radiation.

Solar radiation received by the fraction of the water's surface shaded by vegetation is

determined for shadows cast by each zone as follows:

The Solar radiation flux in the shade of vegetation is calculates as:

$$\Phi_{shadedVegetation} = \Phi_{SRA} \cdot \alpha_{shadedSunward} \cdot \left(1 - Shadow_{densitySunward}\right)$$ **2.27**

Solar radiation on the unshaded fraction of the stream's surface is calculated as:

$$\Phi_{unshadedFraction} = \Phi_{SRA} \cdot (1 - \alpha_{shaded})$$ **2.28**

where the total fraction shaded is the sum of the fractions shaded by the bank and

sunward vegetation.

Direct beam short-wave solar radiation routed to the stream surface is calculated
as the sum of the solar radiation flux received by the shaded and unshaded fractions of
the water's surface:

$$\Phi_{SRV} = \Phi_{shadedVegetation} + \Phi_{unshadedFraction}$$ **2.29**

Recall that a fraction of diffuse solar radiation will arrive at the stream's surface through
the canopy opening. The remaining fraction of diffuse radiation is assumed to be blocked
by the stream bank and bank vegetation. The fraction that reaches the water's surface is
proportional to the fraction of a 180 degree view that is unobstructed by vegetation. This
fraction is the View_To_Sky. The minimum open sky view for each bank VTS_{Bank} is
used in determining the amount of radiation that arrives through riparian vegetation or the
canopy opening. The open sky view is the sum of the minimum open sky view for the
right and left halves of the channel cross-section.

$$VTS_{Bank} = \frac{180}{\pi} \cdot \tan^{-1}\left(\frac{VHeight_{apparent}}{transverse(z)}\right)$$ **2.30**

where $transverse(z)$ equals the distance from the center of the stream to the leading edge
of the zone.

The fraction of a 180° field of view that is open to the sky is calculated as follows:

$$View\_To\_Sky = \frac{VTS_{Bank1} + VTS_{Bank2}}{180}$$ **2.31**

The amount of diffuse solar radiation reaching the water's surface through the canopy
opening is calculated as follows.

$$\Phi_{SDVO2} = \Phi_{SDA} \cdot View\_To\_Sky \qquad\qquad \textbf{2.32}$$

The total of Direct and Diffuse Solar Radiation Passing Water's Surface is:

$$\Phi_{TDS} = \Phi_{SRW} + \Phi_{SDVO2} \qquad\qquad \textbf{2.33}$$

Long Wave (Thermal)

Recall that the long-wave radiation reaching the water's surface is calculated as the sum of radiation through the canopy opening and through streamside vegetation calculated separately. Long-wave radiation through the canopy opening is determined separately for the right and left halves of a channel crossection. The equations used for the right and left banks respectively are:

$$CSR = 0.5 \cdot View\_To\_Sky \cdot (1 - (1 - 0.9 \cdot VegDensityR))^{Veg_{width}} \qquad\qquad \textbf{2.34}$$

$$CSL = 0.5 \cdot View\_To\_Sky \cdot (1 - (1 - 0.9 \cdot VegDensityL))^{Veg_{width}} \qquad\qquad \textbf{2.35}$$

where *VegDensityR* equals the density of vegetation on the right bank and *VegDensityR* is the density of vegetation on left bank.

$$\Phi_{longwaveVegO} = \left[1 - \left(\frac{CSR + CSL}{180} \right) \right] \cdot \left(\Phi_{LongwaveATM} \right) \qquad\qquad \textbf{2.36}$$

The description of the View_To_Sky parameter is described in Equations 2.30 and 2.31.

We would like the term:

$$\left[1-\left(\frac{CSR+CSL}{180}\right)\right]$$

to range from a number close to zero, when the Veiw_To_Sky is zero, to a value close to

1 when the View_To_Sky is 1. The maximum value for both CSR and CSL is 0.5. The

maximum value for the term:

$$\left(\frac{CSR+CSL}{180}\right)$$

is

$$\left(\frac{1}{180}\right)$$

so the minimum value for the term:

$$\left[1-\left(\frac{CSR+CSL}{180}\right)\right] \text{ is } \left[1-\left(\frac{1}{180}\right)\right]=0.995.$$

The value of the term:

$$\left[1-\left(\frac{CSR+CSL}{180}\right)\right]$$

ranges from 0.995 to 1. This equation was adapted as described in Equation 3.27.

Long-wave radiation emitted by riparian vegetation is calculated as:

$$\Phi_{longwaveVeg} = \left[0.95 \cdot \left(\frac{CS0 + CS1}{180} \right) \cdot 0.95 \cdot \sigma \cdot \left(T_{air} + 273.2 \right)^4 \right] \qquad \textbf{2.37}$$

The total atmospheric long wave radiation flux at the water's surface is calculated as the sum of long wave radiation from vegetation and the canopy opening.

$$\Phi_{longwave(+)} = \left(\Phi_{longwaveVeg} + \Phi_{longwaveVegO} \right) \qquad \textbf{2.38}$$

Stream Bed Conduction

Heat Source Version 6 methodology includes an energy balance on the stream bed, where the fraction of the stream bed composed of bedrock may absorb solar radiation routed through the water column. A fraction of this absorbed energy may be transferred back to the water column.

$$\Phi_{TSB} = \Phi_{TDS} \cdot \left(Trans_{stream} \right)^{PLwater} \qquad \textbf{2.39}$$

Solar radiation reaching the stream bed may be absorbed by bedrock and a fraction of the energy absorbed may again be re-absorbed by the water column. The solar flux absorbed by the bed is described as follows:

$$\Phi_{absorbed} = \frac{\Phi_{TSB} \cdot 0.53 \cdot BEDROCK}{100} \qquad \textbf{2.40}$$

The above model for the absorption and radiation of heat energy by stream bedrock was developed by Sellers (1965) and cited by Beschta (1984) and others. The conduction flux, returning stored bed energy to the water column is then calculated as follows:

$$\Phi_{conduction} = \frac{E_{bed}}{14400} \tag{2.41}$$

where $\Phi_{conduction}$ is the conduction flux for one minute of the day (cal/m^2).

The stream bed energy balance is represented by the balance of incoming solar radiation energy absorbed, and conduction flux returned to the water column.

$$E_{bed} = \left(\Phi_{absorbed} - \Phi_{conduction}\right) \cdot dt \tag{2.42}$$

where E_{bed} is the energy stored in the bed (cal/m^2).

Flow Model

Heat Source 6 uses the Manning equation to estimate flow velocity and depth at every distance step given discharge and assumed channel wetted width. The model assumes a rectangular channel. The wetted width is assumed to be equal to 80% of the measured Near Stream Disturbance Zone (NSDZ) width. The NSDZ width is the width that can be measured between vegetal clearings on the channel bank left as evidence of high flows. Measured flow values for each distance step are defined user inputs.

Figure 2.2 Water column and channel cross-section dimensions for Manning's flow model
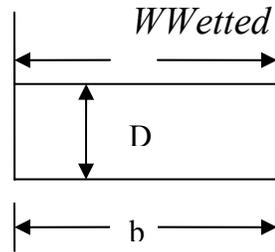
Assuming that the hydraulic radius can be approximated by the depth of flow and the wetted perimeter can be estimated by the top width, Manning's equation for flow can be rearranged as:

$$D = \left[\frac{Q \cdot n}{\delta \, S^{1/2} \cdot WWetted} \right]^{3/5} \qquad\qquad \textbf{2.43}$$

where Q is the discharge (m^3/second), δ is a units conversion factor equal to 1.0 for metric units, S is the channel gradient (dimensionless), n is Manning's roughness coefficient, and $WWetted$ is the water top width (meters) assumed to be given by:

$$WWetted = 0.8 \cdot NSDZ \qquad\qquad \textbf{2.44}$$

Similarly, the flow velocity (meters/second) in the longitudinal x-direction (V_x) is given by:

$$V_x = \frac{\delta}{n} \cdot R^{2/3} \cdot S^{1/2} \qquad\qquad \textbf{2.45}$$

where R is the hydraulic radius (meters) as given by:

$$R = \frac{area}{wetted\ perimeter} \approx D \qquad \textbf{2.46}$$

Assuming a rectangular channel, the general equation describing the change in temperature due to the energy flux from the environment and advection from the upstream element is:

$$\frac{\partial T}{\partial t} = -V_x \cdot \frac{\partial T}{\partial x} + \frac{\Phi_{total}}{\rho_{water} \cdot c_p \cdot D} \qquad \textbf{2.47}$$

where T is the water temperature °C, t is time, ρ_{water} is the density of water (kg/m^3), $c_{p(water)}$ is the heat capacity of water (cal/kg-°C), V is the volume of water (m^3), A is the area associated with the heat flux (m^2), Φ_{total} is the total heat flux (cal/m^2-min), and D is the watercourse depth (m).

CHAPTER 3
METHODS

Study Area

Figure 3.2 presents a map of the Agricultural Production Districts (APD) within King County Washington. The watercourses that drain excess flood water from King County's agricultural land are a combination of constructed drainage ditches and natural or channelized streams. Agricultural drainage watercourses are typically low gradient within the flood plains of various valleys.

Figure 3.1 Map of King County Agricultural Production Districts (APD)
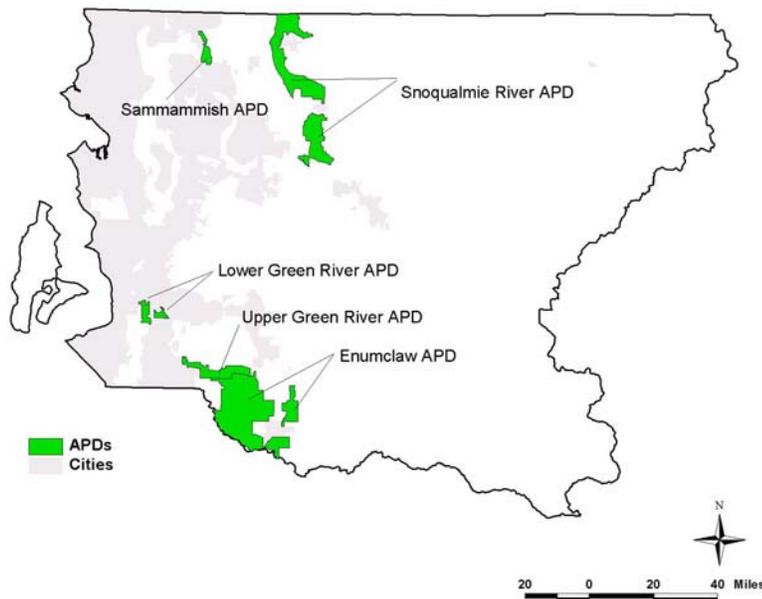
Typical flow conditions in King County's agricultural drainage watercourses are characterized by winter flooding of agricultural land followed by low summer flows obstructed by emergent reed canarygrass and accumulated sediment. Riparian areas have been extensively modified over the years and invasive reed canarygrass is dominant in many locations, although sections of some watercourses still maintain up to 90% native

vegetation (U.S. Army Corps Of Engineers, 1997). Native plant species that grow in the region include Pacific willow (*Salix lasiandra*) and Sitka willow (*Salix sitchensis*), Black cottonwood (Populus trichocarpa), common cattail (*Typha latifolia*), Sedge (*carex retrorsa*), Red-osier dogwood (*Cornus stolonifera*), common horsetail (*Equisetum avense*), Scouring rush (*Equisetum hyemale*), Giant horsetail (*Equisetum telmateia*), and Fecsue (*Festuca sp.*).

The size and dimensions of riparian vegetation are two factors that determine its effectiveness in providing shade. The height of vegetation as well as its proximity to the water's edge and the length of overhang from the stream bank over the water's surface, are factors that determine the amount of the water surface that vegetation will shade. Sitka willows more than eight years old were measured to have both a height and diameter of approximately 5 meters. Sitka willows growing successfully two years following planting were measured approximately 1.8 meters tall and 1.5 meters in diameter. Himalayan blackberries growing along watercourses were measured to be approximately 1.5 meters tall and 4 meters in width. Reed canarygrass was found growing on watercourse banks approximately 1.2 meters tall and often occupying most of the adjacent farm land. Reed canarygrass may grow emergent across the entire watercourse width, grow in a mat over the surface, or grow on the bank, with an overhang distance measured to be approximately 0.3 meters.

King County's climate is moderate and moist. Annual rainfall is approximately 35" per year with light stable rainfall continuing throughout the rainy season from

October through April. The average summer temperature is 64 °F with temperatures rising over 90 °F only a few days per year. Winter temperatures rarely drop below freezing (http://www.enterpriseseattle.com/Research_Data/quality_living.cfm).

Site Selection and Field Data Collection

Field data was collected at sites representing various vegetation types in order to validate the temperature model. For the purposes of model validation and simulation, the focus of this study is limited to summer months when flood flows have typically receded. Water quality is most critical during the summer, when air temperatures are the highest, and flows are lowest. This period represents the greatest potential risk to habitat quality for salmonid fish. During these low-flows, water is generally moving at slow velocities, less than 1 foot per second, and is contained within watercourse banks where it exposed to the effects of riparian vegetation in full foliage rather than occupying the agricultural flood plain. As a result, the same period that represents the greatest risk to salmonid habitat also represents the time when vegetation planted during mitigation may benefit water quality the most.

Study reaches were selected on the basis of relatively uniform water course width, depth, and vegetation type for a minimum length of 100 meters. Reaches were selected with willows, blackberry, or reed canarygrass growing uniformly along the banks. Because the availability of uniform reaches was limited, channel dimensions such as side slope, width and depth were not selected. The morphology of selected reaches was controlled by the vegetation and uniformity criteria. The maximum reach length studied

was 380 meters. Field monitoring included the on site collection of weather data, including direct solar radiation, relative humidity, wind speed and air temperature. Air temperature was collected in association with a weather station located on site as well as by Onset Optic Stowaway temperature sensors located in the shade of riparian vegetation. Stream temperature was collected by installing temperature sensors above and below study reaches in the shade of riparian vegetation. Stream discharge was estimated using a Sontek Flow Tracker to measure velocity. Channel morphology information was collected through field measurements as well as survey data collected by King County. Local topographic shade angles were estimated using topographical maps. The dimensions of riparian vegetation were measured using a measuring tape.

Effective shade cast by vegetation was measured using a Solar Pathfinder below vegetation but above the channel's bankfull height at the mid point of the water's surface. Effective shade was greater than 90% for the reaches studied. Solar radiation was also measured under the vegetation canopy at bankfull level using a CM2 Campbell Scientific pyranometer. Pyranometer measurements were made above the mid point of the water's surface. Reaches were broken into 20 meter segments for pyranometer measurements. At the mid point of each segment a grid approximately 20 inches square, was used to select the position of pyranometer measurements. The grid contained 25 numbered cells. Pyranometer measurements were made below vegetation at cell positions according to a pre-made list of random cell numbers ranging 1 to 25. Measurements were made at a single grid location for approximately fifteen minutes. A corresponding measurement was then made using the same method, outside of the narrow riparian buffer to determine

potential solar exposure. The average of solar radiation measurements made inside and outside of the vegetated buffer for each 20 meter segment was used to approximate effective shade. The approximate location of experimental reaches are highlighted in yellow in the following site maps.

Figure 3.2 Heat Source Model Validation Site 1 Map
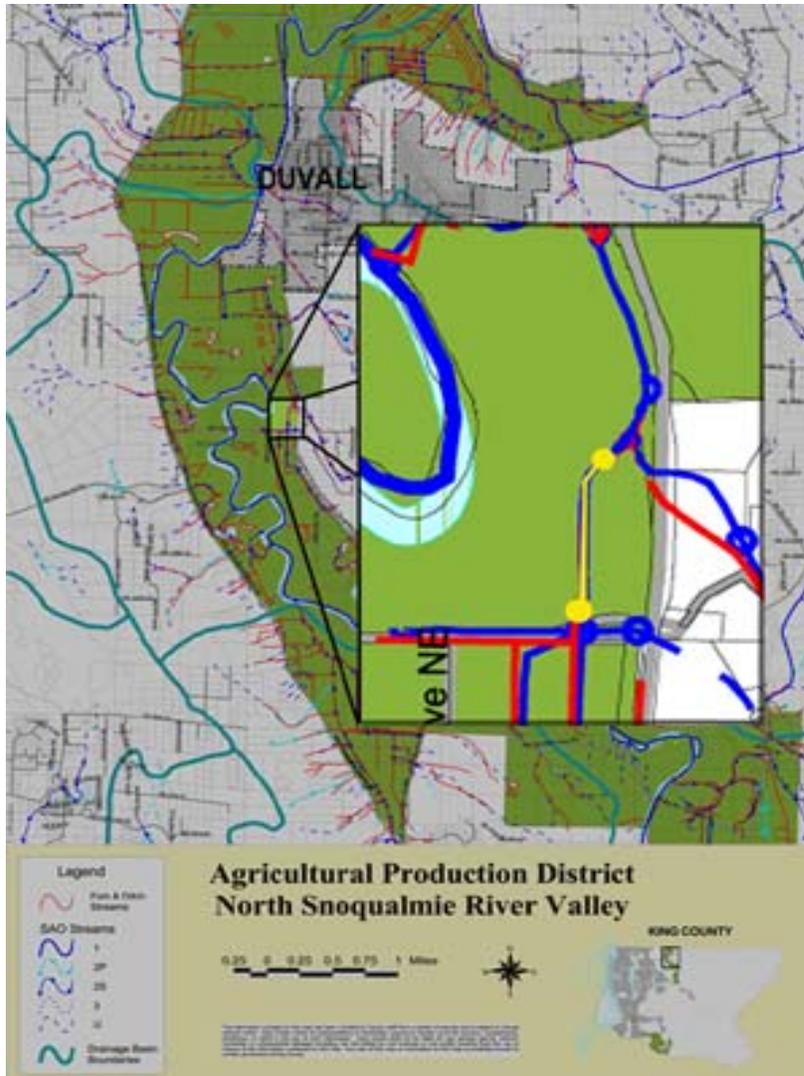
Figure 3.2 shows a map of the approximate location of a validation reach located South of the city of Duvall Washington. The site had reed canarygrass vegetation growing both emergent and on the banks. This reach is approximately 360 meters in

length and demonstrated characteristic slow flows found in obstructed low gradient

watercourses. A small tributary to the site was unmonitored during validation,

representing unknown error. The tributary was visibly contributing no flow during the

short period of temperature validation.

Figure 3.3 Modified Heat Source Model Validation Site 2 Map
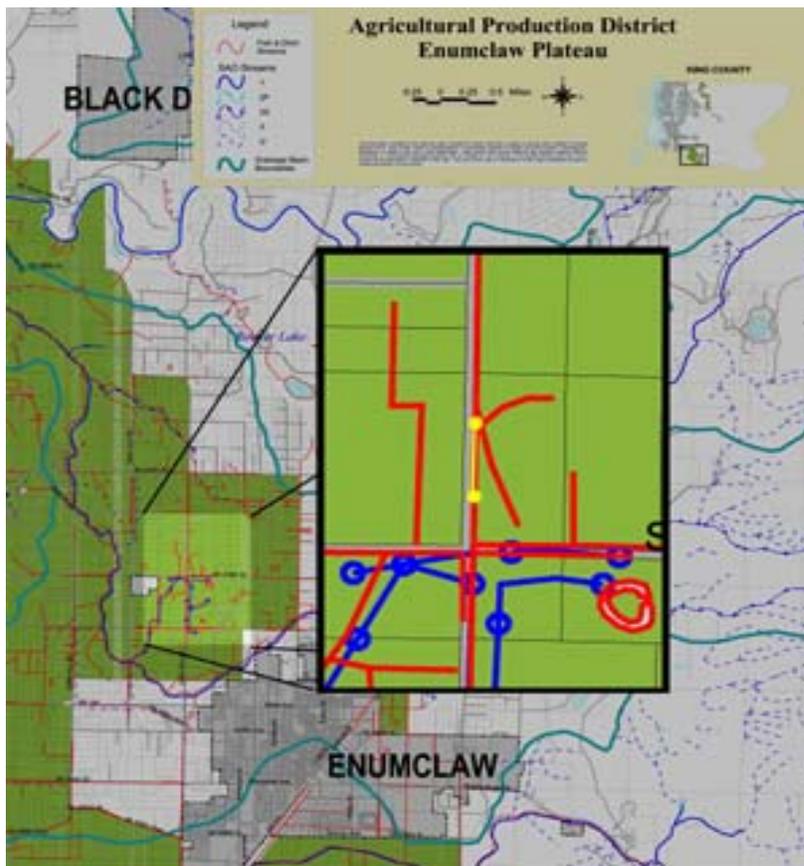
Figure 3.3 shows a map of the approximate location of a reach used for model

validation located North of Enumclaw Washington. This site had mature willows

growing along one bank. The overhang from these willows reached completely across the

water's surface to the opposite bank, providing shade throughout the day. Local

landowners indicated that the willows were approximately eight years old. The distance

between willows at their base varied between approximately six feet and approximately two feet, however, apparent branch and leaf density was relatively uniform throughout the reach indicating that foliage occupied the reach more uniformly than the spacing of plantings. This reach was approximately 100 meters in length.

Figure 3.4 Modified Heat Source Model Validation and Development Site 3

Figure 3.4 shows a map of a site used for validation located South of Kent Washington. This site was approximately two hundred meters long and featured reed canarygrass growing both emergent and on the watercourse banks. This site demonstrated the characteristic slow flows and low gradient of an obstructed watercourse. Dense mats of reed canarygrass growing at the water's surface acted as a complete barrier to solar

radiation in some locations along the reach. Typically reed canarygrass grew emergent from the watercourse at high densities.

Field Data Limitations

Watercourse dimensions cannot be precisely defined in obstructed watercourses with dense reed canarygrass and a deep accumulation of fine organic sediment. The watercourse bottom is not visible and difficult to distinguish by feel due to the slow gradation between semi-suspended colloidal matter and settled material. For the purposes of flow velocity measurement and discharge estimates, the wetted width was approximated by the region where visible or measurable flow velocity could be detected. Measured or estimated flow velocities for the months of July and August were less than 1 foot per second in low gradient agricultural drainage watercourses. For modeling purposes, the wetted width potentially receiving radiation through emergent vegetation is the distance between solid vegetated boundaries on either bank. The depth of the bed conducting layer is represented by the depth of accumulated sediment over the firm channel bottom. In July of 2003, stream bed temperature data was collected by planting an Optic Stowaway temperature sensor approximately four inches deep, into the firm channel bottom. 13.7°C average temperature with diurnal sediment temperature fluctuation of approximately 0.3°C was observed.

Adaptations to the Model Heat Source

Heat Source version 6 was selected as the base model in this study to determine differences in the effectiveness of various riparian vegetation types in providing

watercourse shade and the impact of shading vegetation on watercourse temperature. Research was conducted on a reach scale, monitoring water temperature above and below selected reaches. Reaches were selected and distinguished on the basis of uniformity, each representing a single type of relatively uniform vegetation and the greatest possible uniformity in channel width and depth. Heat Source methodology was customized to predict temperature in small low-gradient watercourses with a minimum of input data for reach-scale mitigation projects. Onsite air temperature and instream water temperature measured above and below each reach was used for validation and development. The Manning's equation flow model in Heat Source 6 was altered to represent a trapezoidal channel with user defined dimensions since project design for maintenance and mitigation projects requires a specified channel side slope. The model is intended for use in identifying the impacts of various changes to watercourse characteristics associated with maintenance of agricultural drainage watercourses. The assumption of relative uniformity in reach-scale characteristics is representative of the test reaches selected and allows the system to show a response to one condition applied uniformly. A wetland Manning's flow model was incorporated into the model to represent obstructed low gradient channels, and adjustments were made to the shade model to best represent the shade cast by small stands of vegetation along small slow flowing watercourses.

The primary user interface for the modified model is the Inputs worksheet. The first column on the worksheet presents a set of labeled input cells where fixed input data including reach length, simulation start date, reach latitude, reach longitude, reach aspect, reach elevation, riparian zone width, channel side slopes, channel bottom width, water depth, channel incision, topographic shading angles to the West, South, and East,

Manning parameter, channel slope, and simulation duration are entered. The user must then select a type of vegetation from the drop down box for the right and left channel banks as observed when looking upstream. To select the wetland flow model, the check box labeled "channel obstructed by reed canarygrass" should be checked by the user. If emergent reed canarygrass is providing watercourse shade, the check box labeled "Emergent veg" should be checked by the user. The default type of emergent vegetation is reed canarygrass. To change the variety of emergent vegetation used in simulation, the user must go to the Riparian Code worksheet and identify the code that represents the desired vegetation type. This value is entered into the white data entry box below the label "Emergent Veg Code". When all input data has been supplied to white input data cells on the Inputs worksheet, the user should press the "Reset" command button to prepare the model for a new simulation. The "Run Vegematic" command button fills the code for the selected vegetation type into data input locations on the Main Menu worksheet representing vegetation for the first distance step. These values are simply automatically copied down to all distance steps on the Main Menu. Vegematic then reads the vegetation code from the main menu and fills the appropriate height, density and overhang values into the rest of the Main Menu riparian data locations. The next executable button on the Inputs worksheet takes the user to the Continuous Data worksheet. The location (distance from the upstream boundary) of each continuous data node (the point of weather data collection) must be specified. Wind speed, relative humidity and air temperature must be provided on an hourly basis throughout the simulation period. Simulation begins at midnight on the first day and the continuous weather data record provided must begin at midnight on the first simulation day. Water

temperature may be provided at each continuous data node for validation but is not required. To return to the Inputs worksheet, the user can select the inputs tab or click on the "Finish and Return to Inputs" command button at the top of the Continuous Data worksheet. The next command button on the Inputs worksheet is the "Input Initial Conditions" button. The required initial conditions are the water temperature values at midnight of the first simulation day for each distance step. When data input is complete, the model methodology is executed by clicking the next button "Start Simulation".

Heat Source Version 6 was designed as a daily model, accepting one day's continuous data and reporting one day's simulation results. It has been adapted to accept ongoing continuous data over several days. At the end of a simulation day, the model was originally designed to present only one day's results. The modified model maintains a record of simulated stream temperatures over the period of simulation as well as solar fluxes above and below riparian vegetation over the course of simulation on a fifteen minute basis. Records of output parameters recorded on a fifteen minute basis are located on the "Validation" worksheet. Following is a review of the model equations used in Heat Source 6 and discussion of model adaptations.

Recalling equation 2.2, the temperature change due to net heat flux from the environment was simplified for a rectangular channel. This simplification no longer applies when modeling a trapezoidal channel with defined side slopes. The temperature change due to environmental heat flux is calculated according to:

$$\frac{\partial T}{\partial t} = -V_x \cdot \frac{\partial T}{\partial x} + \frac{\Phi \cdot A_s}{\rho_{water} \cdot c_p \cdot V} \qquad \textbf{3.1}$$

where ΔT is the change in temperature for a single distance step during the simulation minute (°C), Φ is the net heat energy flux occurring for one minute (cal/m^2), ρ is the density of water (kg/m^3), c_p is the heat capacity of water (cal/kg-°C), A_s is the stream surface area (m^2), and V is the volume of water in the element (m^3). Field observations of Sitka willows planted for the purpose of mitigation after watercourse maintenance showed that willows planted on only one bank may provide complete cover for a narrow watercourse. Modifications were made to the model heat source to describe vegetation that provided extreme overhang and cover.

Short Wave Solar Radiation

In the modified model, vegetation that is strictly bank vegetation exists in only in Zone 1, which has a user defined width perpendicular to the water's edge. Zone 1 is the outermost zone, reaching from the bankfull edge onto adjacent land. Overhanging vegetation is that length of vegetation growing in Zone 1 that extends beyond the bankfull edge, over the sloping bank or the water's surface. Zone 0 is the bank of the watercourse, its width is the model calculated distance between the water's edge and the bankfull edge. This width is based on calculated wetted width and user defined channel side slopes. The first calculation is the average distance from the bankfull mark to the water's edge. This equation assumes that the transverse distances from the water's edge to bankfull are equal on both banks.

49

$$Transverse_0 = \frac{Bankfull_{Width} - Wetted_{Width}}{2}$$

<div align="right">3.2</div>

where $Transverse_0$ is the distance from the water's edge to the bankfull edge (meters).

To calculate solar radiation received at the water's surface, the sunward bank is identified using a comparison of defined stream aspect and calculated solar azimuth angles. The length of shadow cast by the sunward bank itself is first approximated:

$$Shadow_{widthBank} = \frac{Incision \cdot \sin\left|\theta_{azimuth} - \theta_{aspect}\right|}{\tan \theta_{sun}}$$

<div align="right">3.3</div>

where $Incision$ is the vertical distance that the bank extends above the water's surface. The incision distance is a field measured model input. The length of shadow cast by the stream bank that exists only on the water's surface is this shadow length minus the transverse distance. If the shadow length minus the transverse distance is greater than the wetted width, the fraction of the water's surface covered by the bank's shadow is set to 1.

After the length of shadow cast by the bank has been determined, the length of shadow cast by vegetation on the sunward bank and by overhanging vegetation growing on the opposite bank are determined. Excepting emergent and overhanging vegetation, vegetation is assumed to exist at the top of the bank at bankfull elevation above the water's surface. Its distance from the water's edge is calculated based on field measured channel dimensions and calculated wetted width. Riparian vegetation may overhang

from the bankfull edge and overhang the stream's surface. If overhanging vegetation does not overhang the water's surface, the transverse distance from the water's edge to the leading edge of riparian vegetation is calculated as follows:

$$Transverse_1 = Transverse_0 - Veg_{Overhang} \qquad\qquad \textbf{3.4}$$

The model has been adapted so that if the overhanging length is greater than the transverse distance $Transverse_0$ to the water's edge, then the vegetation overhangs the water's surface.

$$Overhang_{length} = \left| Transverse_0 - Veg_{Overhang} \right| \qquad\qquad \textbf{3.5}$$

Vegetation existing only on the bank is considered separate from the portion of vegetation that is overhanging. Because of this distinction the transverse distance from the water's edge to the leading edge of bank vegetation is set to the bank transverse distance.

$$Transverse_1 = Transverse_0 \qquad\qquad \textbf{3.6}$$

The length of shadow cast by vegetation on the sunward bank at distance $Transverse_0$ from the water's edge is calculated. The model is adapted so that this shadow length is transformed by the value of the overhang length, to represent the shadow cast from the edge of the overhang based on Chen (1998).

51

$$Shadow_{width} = \frac{VegH_{apparent} \cdot \sin\left|\theta_{azimuth} - \theta_{aspect}\right|}{\tan\theta_{sun}} + Overhang_{length}$$ **3.7**

The shade density of a shadow cast by riparian vegetation is calculated by first estimating a riparian extinction coefficient for the vegetated zone according to the methodology described by Chen et al (1998). If the length of the shadow cast by riparian vegetation on the sunward bank is greater than the transverse distance and greater than the shadow cast by the bank, then a fraction of the streams surface is shaded only by vegetation. Heat Source 6 methodology is adapted so that the shadow from vegetation on the sunward bank may overlap with the shadow cast by overhanging vegetation on the opposite bank. The shadow cast by overhang from the non-sunward bank begins at the sunward edge of overhanging vegetation, over the water's surface. The shadow will be cast toward the non-sunward bank from the position of the leading edge of overhang over the water's surface. The length of a shadow cast by overhanging vegetation on the opposite bank is approximated as:

$$Shadow_{OverhangOpposite} = OverhangLength - \frac{Incision \cdot \sin\left(\theta_{azimuth} - \theta_{aspect}\right)}{\tan\left(\theta_{solar}\right)}$$ **3.8**

The length of this shadow over the water's surface is the shadow length minus the transverse distance to bankfull, which is included in the overhang length. The shadow

52

density cast by vegetation is a function of the density of vegetation and the path length through vegetation as described by Chen (1998).

$$\lambda = -\frac{Ln(1 - VegDensity)}{VegH_{actual}}$$ **3.9**

where λ Riparian extinction Coefficient (m^{-1}), VegDensity is typically estimated from aerial photographs as the percentage of land in the riparian zone occupied by vegetation (dimensionless), $VegH_{actual}$: Height of riparian vegetation (meters), Veg_{width} is the width of vegetation from bankfull edge perpendicular to the bank (meters), and PL_{veg} is the approximated path length of solar radiation through riparian vegetation (meters).

The path length approximation follows methods outlined by Boyd (2004) for riparian and emergent vegetation. Before the sun's altitude angle reaches the top of riparian vegetation:

$$PL_{veg} = \frac{Veg_{width} + Veg_{overhang}}{\left| \sin \left| \theta_{azimuth} - \theta_{aspect} \right| \right| \cdot \cos \theta_{sun}}$$ **3.10**

When the sun is overhead of overhanging or emergent vegetation:

$$PL_{vegOver} = \frac{Veg_{height}}{\sin \theta_{sun}}$$ **3.11**

The density of the shadow cast by vegetation is determined based on Beer's Law according to Chen (1998).

$$Shadow_{density} = 1 - e^{\left(-\lambda \cdot PL_{veg}\right)} \qquad\qquad\qquad \textbf{3.12}$$

The water's surface may be shaded by the sunward bank's vegetation only, both banks' vegetation at once, the sunward bank itself, or overhanging vegetation from the opposite bank only. The fraction of the water's surface shaded by the bank receives no solar radiation, in a manner similar to that described by Boyd (2004). Solar radiation received by the fraction of the water's surface shaded by vegetation is determined as follows:

$$\Phi_{shadedVegetation} = \Phi_{SRA} \cdot \alpha_{shadedSunward} \cdot \left(1 - Shadow_{densitySunward}\right) \qquad\qquad \textbf{3.13}$$

$$\Phi_{shadedOverhang} = \Phi_{SRA} \cdot \alpha_{shadedOverhang} \cdot \left(1 - Shadow_{densityOverhang}\right) \qquad\qquad \textbf{3.14}$$

The shadow from vegetation on the sunward bank may overlap with the shadow cast by overhanging vegetation on the opposite bank. Solar radiation reaching the fraction of the surface shaded by overlapping shadows is calculated as:

$$\Phi_{shadedOverlap} = \Phi_{SRA} \cdot \alpha_{shadedOverlap} \cdot \left(1 - Shadow_{densitySunward}\right) \cdot \left(1 - Shadow_{DensityOverhang}\right) \quad \textbf{3.15}$$

The total solar flux reaching the shaded fraction of the wetted width is the sum of solar radiation through bank vegetation, overhanging vegetation, and the overlap of shadows from both.

$$\Phi_{shadedFraction} = \Phi_{shadedOverlap} + \Phi_{shadedVegetation} + \Phi_{shadedOverhang} \qquad \textbf{3.16}$$

Solar radiation on the unshaded fraction of the stream's surface is calculated as:

$$\Phi_{unshadedFraction} = \Phi_{SRA} \cdot (1 - \alpha_{shaded}) \qquad \textbf{3.17}$$

Where the total fraction shaded is the sum of the fractions shaded by the bank, the sunward vegetation only, overhanging vegetation from the opposite bank only, and the fraction shaded by vegetation from both banks at once.

Direct beam short-wave solar radiation routed to the stream surface is calculated as the sum of the solar radiation flux received by the shaded and unshaded fractions of the water's surface.

$$\Phi_{SRV} = \Phi_{shadedFraction} + \Phi_{unshadedFraction} \qquad \textbf{3.18}$$

Where emergent reed canarygrass is present, direct beam short-wave solar radiation is next routed through emergent vegetation. Emergent vegetation is assumed to be of uniform density across the water's surface. The shade density for emergent vegetation is estimated according to the same relationships used for bank vegetation, and the path length is estimated according to the same relationship described for bank vegetation when the sun is overhead as presented by Boyd (2004).

The total of Direct and Diffuse Solar Radiation passing water's surface is:

$$\Phi_{TDS} = \Phi_{SRW} + \Phi_{SDVO2} \qquad\qquad\qquad \textbf{3.19}$$

The Net Solar Radiation Flux is:

$$\Phi_{solar} = \Phi_{SRW} + \Phi_{DRW} - \Phi_{absorbed} = \Phi_{TDS} - \Phi_{absorbed} = \Phi_{TDS} \qquad\qquad \textbf{3.20}$$

Long Wave (Thermal)

Recall that emitted long-wave solar radiation reaching the water's surface is a function of canopy closure over the stream. Modifications have been made to the determination of canopy closure or open sky view (View_To_Sky) to best represent extensively overhanging vegetation. The open sky view is determined as the sum of open sky view for the right and left banks. To determine the fraction of a 90° field of view that is unobstructed, in the modified model a check is made to determine if overhanging vegetation reaches beyond the mid point of the wetted width for either bank.

If vegetation from neither bank extends beyond the stream mid point, then the view to sky for each half of a channel cross-section is calculated as:

$$VTS_{Bank} = \frac{180}{\pi} \cdot \tan^{-1}\left(\frac{VHeight_{apparent}}{\dfrac{WWidth}{2} - OverhangLength} \right) \qquad\qquad \textbf{3.21}$$

The open sky view is zero in the case of complete overhang from both banks. If overhanging vegetation on one bank reaches beyond the mid point of the stream, then one bank's open sky view is zero, the other is calculated as follows:

$$VTS_{BankS} = 90 - \frac{180}{\pi} \cdot \tan^{-1}\left(\frac{VHeight_{apparentS}}{OverhangLengthS - \frac{WWidth}{2}}\right)$$

$$- \frac{180}{\pi} \cdot \tan^{-1}\left(\frac{VHeight_{apparent}}{\frac{WWidth}{2} - OverhangLength}\right) \qquad \textbf{3.22}$$

The fraction of a 180° field of view that is open to the sky is calculated as follows presented by Boyd et al (2004):

$$View\_To\_Sky = \frac{VTS_{Bank1} + VTS_{Bank2}}{180} \qquad \textbf{3.23}$$

Long-wave radiation reaching the water's surface is calculated as the sum of radiation through the canopy opening, and through streamside vegetation calculated separately. Long-wave radiation through the canopy opening is described by:

$$\Phi_{longwaveVegO} = \left[View\_To\_Sky\right] \cdot \left(\Phi_{LongwaveATM}\right) \qquad \textbf{3.24}$$

Long-wave radiation emitted by riparian vegetation as presented by Boyd et al (2004)

$$\Phi_{longwaveVeg} = \left[0.96 \cdot \left(1 - View\_To\_Sky\right) \cdot 0.96 \cdot \sigma \cdot \left(T_{air} + 273.2\right)^4\right] \qquad \textbf{3.25}$$

57

Because the stream bank itself may restrict the open sky view when the channel is incised, the modified model subtracts the bank angle from (1-View_To_Sky) when calculating long-wave radiation emitted by riparian vegetation.

$$\Phi_{longwaveVeg} = \left[0.96 \cdot \left(1 - View\_To\_Sky - BAngle \right) \cdot 0.96 \cdot \sigma \cdot \left(T_{air} + 273.2 \right)^4 \right]$$ **3.26**

$$BAngle = \left(\frac{2}{\pi} \right) \cdot a\tan\left(\frac{Incision}{\left(\frac{1}{2} \cdot Wwidth \right) + Transverse_0} \right)$$ **3.27**

The total atmospheric long wave radiation flux at the water's surface is calculated as the sum of long wave radiation through vegetation and the canopy opening.

$$\Phi_{longwave(+)} = \left(\Phi_{longwaveVeg} + \Phi_{longwaveVegO} \right)$$ **3.28**

Net long wave radiation balance at the water's surface is the sum of long wave radiation received by the atmosphere and long wave radiation emitted by the stream.

$$\Phi_{longwave} = \Phi_{longwave(+)} + \Phi_{longwave(-)}$$ **3.29**

Stream Bed Conduction

Heat Source Version 6 methodology includes an energy balance on the stream bed, where the fraction of the stream bed composed of bedrock may absorb solar radiation routed through the water column. A fraction of this absorbed energy may be

transferred back to the water column. According to Heat Source 6 methodology, because the low gradient streambeds under consideration have been composed entirely of fine organic material and silt, energy storage by the stream bed would be neglected. The modified model replaces this methodology with methods based on the upgraded bed conduction methods used in Heat Source version 7.0. Soil temperatures are generally cooler and more stable than air or water temperatures. Conduction between the bed and water column is calculated based on the characteristics of the conducting layer according to the fractions of sediment and water that compose the bed. The following is according to Boyd and Kasper (2004).

$$\rho_{bed} = \left(\rho_{seidment} \cdot \alpha_{se\,dim\,ent} \right) + \left(\rho_{water} \cdot \alpha_{water} \right) \qquad \textbf{3.30}$$

$$V_{Hyporeic} = P_{wetted} \cdot D_{se\,dim\,ent} \cdot dx \qquad \textbf{3.31}$$

$$V_{water} = \vartheta_{se\,dim\,ent} \cdot P_{wetted} \cdot D_{se\,dim\,ent} \cdot dx \qquad \textbf{3.32}$$

$$V_{se\,dim\,ent} = \left(1 - \vartheta_{se\,dim\,ent} \right) \cdot P_{wetted} \cdot D_{se\,dim\,ent} \cdot dx \qquad \textbf{3.33}$$

$$\alpha_{se\,dim\,ent} = \frac{V_{se\,dim\,ent}}{V_{Hyporeic}} \qquad \textbf{3.34}$$

$$\alpha_{water} = 1 - \alpha_{se\,dim\,ent} \qquad \textbf{3.35}$$

$$\mathrm{K}_{bed} = \left(\mathrm{K}_{se\,dim\,ent} \cdot \alpha_{se\,dim\,ent} \right) + \left(\mathrm{K}_{water} \cdot \alpha_{water} \right) \qquad \textbf{3.36}$$

$$\Psi = \left(\Psi_{se\,dim\,ent} \cdot \alpha_{se\,dim\,ent} \right) + \left(\Psi_{water} \cdot \alpha_{water} \right) \qquad \textbf{3.37}$$

where ρ_{bed} is the volumetric weighted density (kg/m^3), $\rho_{seidment}$ is the substrate density (typically assumed to be 1600kg/m^3), ρ_{water} is the density of water (kg/m^3), α_{water} is the water volume ratio (dimensionless), $\alpha_{sediment}$ is the sediment volume ratio (dimensionless), $D_{sediment}$ is the depth of the conduction layer (m), K_{water} is the water thermal conductivity (typically assumed to be 0.60 J/ m s °C), $K_{sediment}$ is the sediment thermal conductivity (typically assumed to be 15.98 J/ m s °C), K_{bed} is the volumetric composite thermal conductivity in conduction layer (J/ m s °C), v_{water} is the water volume in conduction layer (m^3), $v_{sediment}$ is the substrate volume in conduction layer (m^3), $v_{Hyporeic}$ is the total volume in conduction layer (m^3), $\vartheta_{sediment}$ is the porosity of the conduction layer (dimensionless), $\Psi_{sediment}$ is the substrate thermal diffusivity (m^2/s), and Ψ_{water} is the water thermal diffusivity (m^2/s).

The heat flux transferred to the water column is calculated:

$$\Phi_{conduction} = \frac{\Psi \cdot \rho_{bed} \cdot K_{bed} \cdot \left(T_{Sediment} - T_{water0} \right)}{\dfrac{D_{sediment}}{2}} \cdot C_{onversionFactor} \qquad \textbf{3.38}$$

$$\Phi_{sediment} = -\Phi_{conduction} \qquad \textbf{3.39}$$

$$\Delta T_{sediment} = \frac{\Phi_{sediment} \cdot P_{wetted} \cdot dx \cdot dt}{\rho_{bed} \cdot K_{bed}} \qquad \textbf{3.40}$$

$$\Delta T_{se\,dim\,ent} = T_{Se\,dim\,ent} + \Delta T_{se\,dim\,ent} \qquad\qquad\qquad\qquad\qquad \textbf{3.41}$$

Flow Model

The modified flow model uses Manning's equation to estimate channel flows. Channel side slope is an important design parameter that impacts bank and riparian vegetation shade. User inputs include water depth, channel bottom width, channel side slope, channel gradient, and Manning's n. The Wetland Manning flow model presented by Crites (1998) has been added to the adapted model as an available as an option to model flow in watercourses heavily obstructed with vegetation. Figure 3.5 is a general diagram illustrating cross-section parameters used in the Manning flow model. Figure 3.5 presents a general diagram illustrating the parameters used to calculate open channel flow for both unobstructed and wetland or obstructed conditions.

Figure 3.5 Water column and channel cross-section dimensions for Manning's flow model
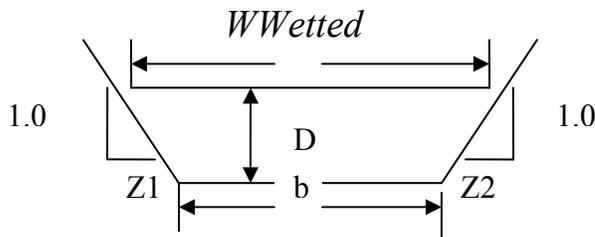
Unobstructed flow is modeled as follows:

$$Q = V_x \cdot A_c \tag{3.42}$$

Where V_x is the flow velocity (meters/second)

$$V_x = \frac{\delta}{n} \cdot R^{2/3} \cdot S^{1/2} \tag{3.43}$$

where R is the hydraulic radius (meters), S is the channel gradient (dimensionless), Q is the discharge (m^3/second), n is Manning's roughness coefficient, A_c is the channel cross-sectional area (m^2), and δ is the conversion factor equal to 1 for metric units

For a trapezoidal channel, R and A_c are calculated as follows:

$$R = \frac{A_c}{P_{wetted}} \tag{3.44}$$

$$A_c = \frac{D}{2} \cdot (b + WWetted) \tag{3.45}$$

where D is the water depth (meters), b is the channel bottom width (meters), and *WWetted* is the water surface width (meters). For a trapezoid:

$$WWetted = b + D \cdot (Z1 + Z2) \tag{3.46}$$

and P_{wetted} is the wetted perimeter (meters)

$$P_{wetted} = b + D \cdot \left(\sqrt{(1 + Z1^2)} + \sqrt{(1 + Z2^2)} \right) \tag{3.47}$$

For wetland, or obstructed flow, a similar equation applies with an adjustment to n according to Crites et al (1998):

$$n = \frac{a}{D^{1/2}}$$

3.48

where a is the resistance factor ($s \cdot m^{1/16}$) defined by:

$a = 0.487$ for sparse vegetation with Y > 1.3 feet

$a = 1.949$ for moderately dense vegetation and Y = 1 foot

$a = 7.795$ for very dense vegetation with a litter layer and Y< 1 foot.

In the wetland Manning's flow model presented by Crites (1998) the hydraulic radius is replaced by water depth and velocity is calculated according to Equation 3.47.

CHAPTER 4
RESULTS

Model Validation

The modified model was validated at four sites representing three vegetation types: 1 Willow site, 2 reed canarygrass sites, and 1 site with no vegetation. Efforts were made to study simplified reaches during low flow conditions when ground water and intermittent variable surface flows would be minimized. Figure 4.1 shows hourly predicted and measured temperature at the downstream end of a site 100 meters in length with willow vegetation overhanging the width of the watercourse. Simulation results for the five day temperature validation simulation resulted in $R^2 = 0.77$, Root mean square error (RMSE) = 0.41. Results for 14 day simulation at the same site resulted in $R^2 = 0.87$, RMSE = 0.63. Figure 4.1 shows hourly predicted and measured temperature at the downstream end of the reach. Figure 4.1 indicates that predicted and measured temperatures in this validation scenario typically differ by less than half a degree.

Figure 4.1 Validation results for the modified Heat Source model with willow vegetation

Figure 4.2 Validation results for the modified Heat Source model with reed canarygrass vegetation
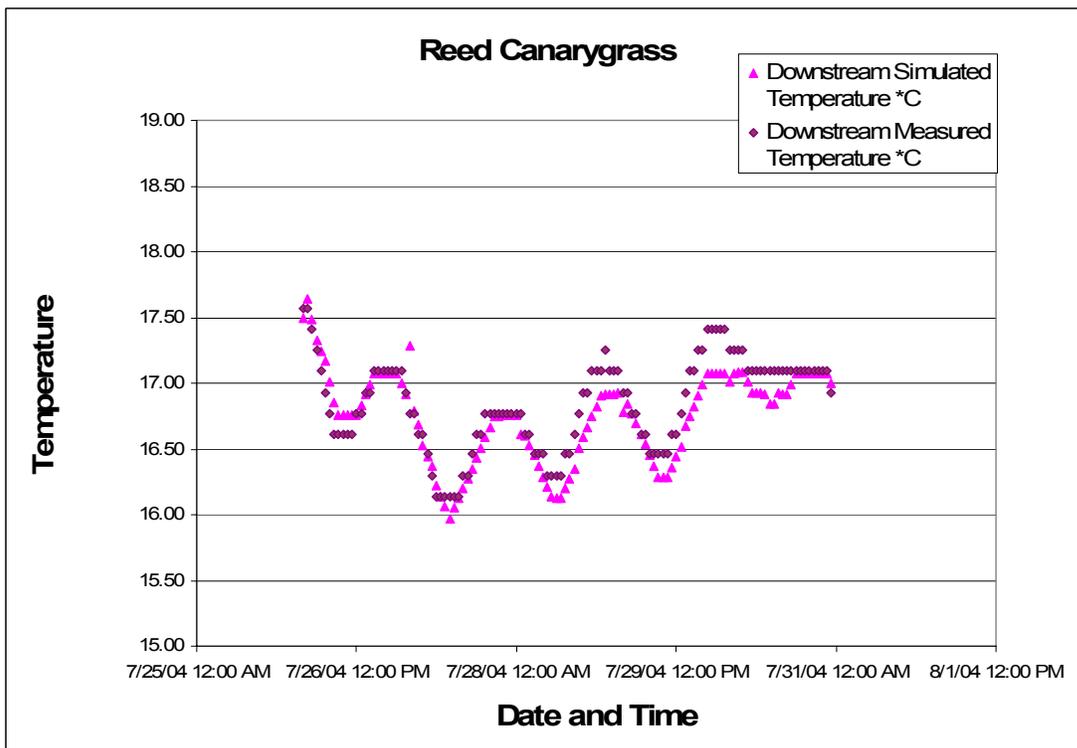
Figure 4.2 shows simulated and measured downstream temperature over a 200 meter reach with reed canarygrass growing on the banks and growing emergent from the watercourse. $R^2= 0.83$ for this simulation and RMSE= 0.17. The modified wetland Mannig's flow feature in the adapted model was used for this simulation. Measured and predicted temperatures for this validation simulation typically differ by less than half a degree.

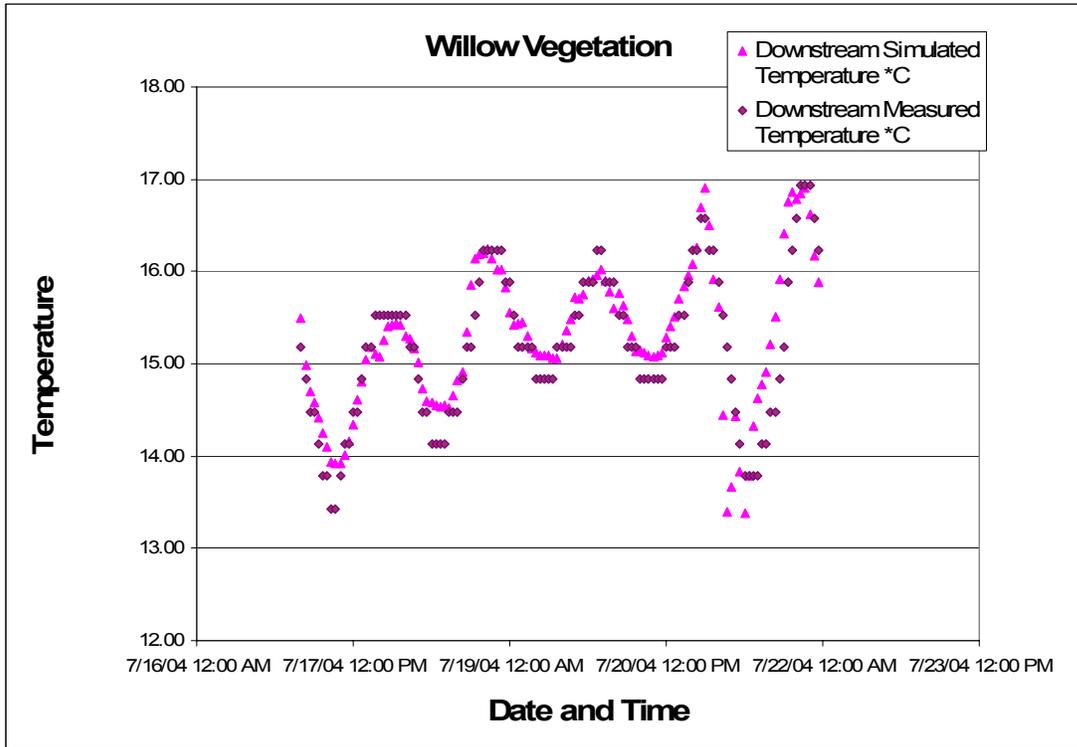**Figure 4.3 Validation results for the modified Heat Source model with no riparian vegetation**
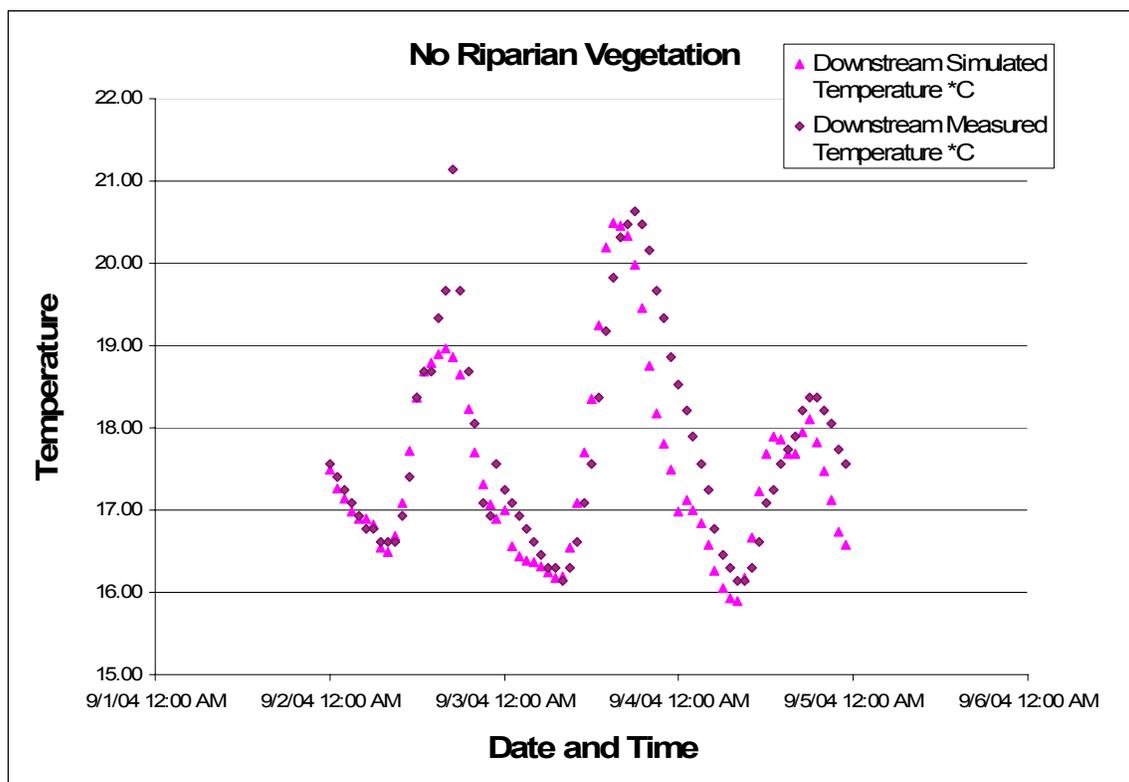
Figure 4.3 shows simulation results for a 100 meter reach that was cleared of vegetation during maintenance. Results for this simulation showed $R^{2 =} 0.76$ and RMSE=

0.68. Measured and predicted temperatures in this validation scenario also typically differ by less than half a degree.

Figure 4.4 shows results from simulation over a reach 360 meters in length with reed canarygrass growing emergent and on the channel banks. This simulation shows greater error compared with results from other validation simulations. This error can be seen in the difference between simulated and measured temperatures, for example close to 12:00 July 17th. Simulation results showed $R^2 = 0.77$, RMSE= 0.65. Although no net change in flow could be measured across this reach, potential sources of model error include un-detected ground water exchange. A small ephemeral tributary to this reach was observed to have zero flow during the validation period, but could have had an undetected subsurface component.

Figure 4.4 Validation results for the modified Heat Source model with reed canarygrass vegetation
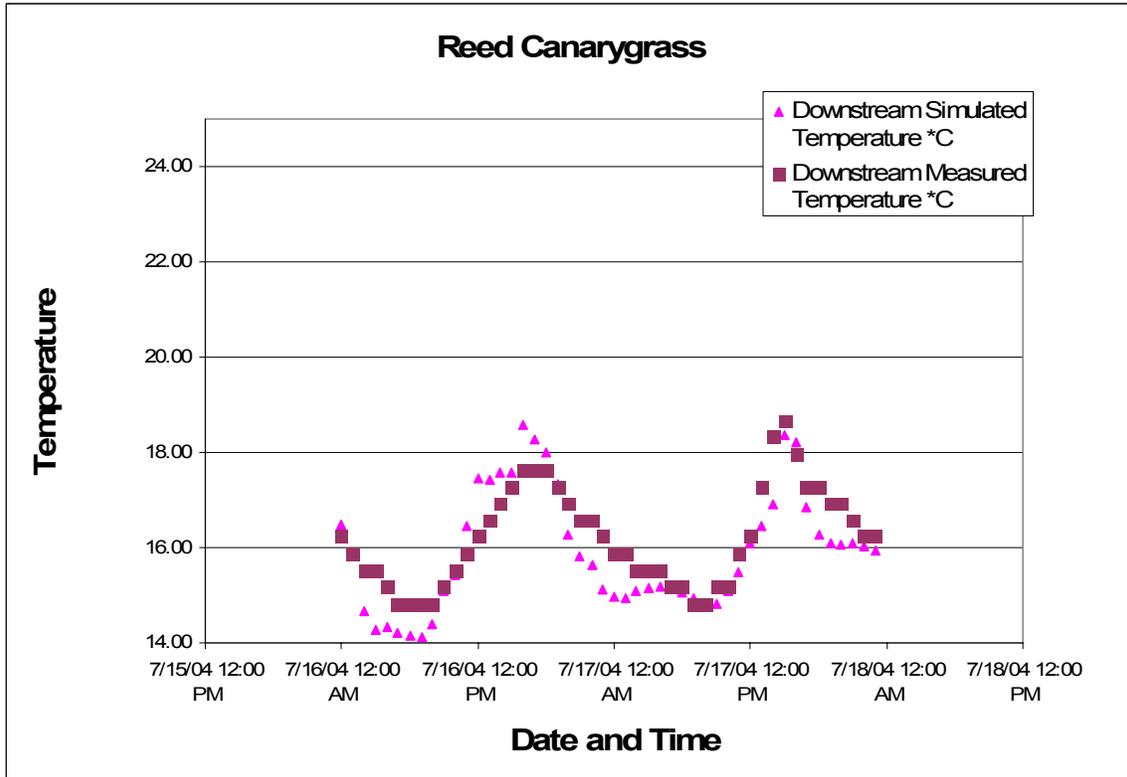
While error is observable in these validation simulations, it is generally less than half a degree. The willow vegetation validation scenario appears to show more error at low temperatures, while Figure 4.2, validation for reed canarygrass, shows most error during high temperatures. Figure 4.3 shows a small amount of temporal offset, indicating that the simulated time of travel may be slower than the actual. No consistent type of error is evident in these validation simulations and error is generally small.

Sensitivity Analysis of Major Design and Management Parameters

The objective of sensitivity analysis is to identify the magnitude of the model's response to individual input data parameters over the practical range of input values. Sensitivity analysis is used to determine the factors that have the greatest proportionality

to system response. The model's response to a change in each input parameter is found by comparing each "test" scenario result with the one "baseline" scenario result. Because model sensitivity may depend on baseline conditions, two baseline scenarios are considered to evaluate model sensitivity over the range of reasonable input values.

Sensitivity analysis is carried out by changing the value of exactly one parameter at a time. For this reason, sensitivity scenarios do not necessarily yield scenario results that are practical from a management perspective. Sensitivity analysis results should not be confused with maintenance scenarios. For example, in a real world scenario, watercourse morphology may be altered to result in decreased watercourse depth, yet the flow in the channel may remain constant, since other watercourse characteristics would have also changed to accommodate the same flow. In a sensitivity analysis scenario, decreasing only watercourse depth results in a smaller calculated flow. Sensitivity analysis results do not necessarily represent the change in temperature that would occur as changes are made to one watercourse, they indicate the sensitivity of the model to input parameters.

Table 4.1 outlines the input parameters used for baseline 1 in sensitivity analysis. The RCG density used for this sensitivity analysis was 93%. This value was selected to make the shadow cast by reed canarygrass at least slightly different from the shadow that would be cast by an opaque object to remain conservative in estimating the sensitivity of the model to reed canarygrass shade. The width of buffer vegetation on the bank was

defined at 2.5 meters. In most observed field conditions the buffer width for vegetation of every kind was at least this wide.

Table 4.1 Baseline 1 parameters for sensitivity analysis

Parameter	Baseline Value	Units
Simulation Period	14	Days
Start date	7/15/04	Date
Lat	42.6	Degrees
Long	-121.6	Degrees
Aspect	180	Degrees
Right Side Slope	2	H:V
Left Side Slope	2	H:V
Incision	0.5	Meters
Bottom width	2.0	Meters
Water Depth	0.15	Meters
Manning's n	0.2	
Channel gradient	0.001	%
Right Bank Vegetation	RCG	
Left Bank Vegetation	RCG	
Sediment Depth	0.5	Meters
Sediment Temperature	13.7	Degrees C

Weather data used in simulation was gathered from the University of Washington rooftop weather station. Online one-minute data is available at http://www-k12.atmos.washington.edu/k12/grayskies/nw_weather.html

Table 4.3 outlines the results of sensitivity analysis simulations for predicted Maximum Seven Day Average of Daily Maximum Temperatures. Changes in parameters including flow depth and side slope also impact simulated discharge and surface area. Consideration of these impacts is useful in analyzing simulation results. For this reason, descriptive parameters such as effective shade and discharge are included in Table 4.2.

Table 4.3 shows the sensitivity coefficient determined for each simulation as the ratio of the percentage change in the maximum seven day average of daily maximum temperature, divided by the percent change in input parameter. Air temperature is the parameter with the highest model sensitivities among all values and parameters tested for this baseline scenario. Air temperature was adjusted by increasing every hourly measured air temperature input value by the number of degrees indicated in Table 4.2.

Table 4.2 Baseline 1 Sensitivity Analysis Results Modified Heat Source

| Test Parameter	Test Parameter Value	Maximum 7-Day Average of Daily Maximum Temperature °C	Discharge	Flow Velocity	Date and Time of Maximum	Depth	Wetted Width	Effective Shade
Baseline		18.3	0.014	0.04	7/23/04 3:00 PM	0.15	2.6	0.20
Side Slope	1:1	18.2	0.013	0.04	7/23/04 3:00 PM	0.15	2.3	0.32
Side Slope	3:1	18.5	0.015	0.04	7/23/04 3:00 PM	0.15	2.8	0.14
Side Slope	2.5:1	18.4	0.014	0.04	7/23/04 3:00 PM	0.15	2.8	0.16
Willow Density	93%	17.6	0.014	0.04	7/23/04 5:00 PM	0.15	2.6	0.90
Willow Density	50%	17.7	0.014	0.04	7/23/04 5:00 PM	0.15	2.6	0.68
Willow Density	20%	18.3	0.014	0.04	7/23/04 3:00 PM	0.15	2.6	0.20
Bank Incision	1.0	18.3	0.014	0.04	7/23/04 3:00 PM	0.15	2.6	0.19
Bank Incision	0.1	17.7	0.014	0.04	7/23/04 4:00 PM	0.15	2.6	0.77
Bank Incision	0.0	17.6	0.014	0.04	7/23/04 5:00 PM	0.15	2.6	0.70
No Vegetation	0	18.4	0.014	0.04	7/23/04 5:00 PM	0.15	2.6	0.06
Water Depth	0.5	18.3	0.120	0.09	7/23/04 4:00 PM	0.50	3.2	0.14
Water Depth	0.1	18.5	0.007	0.03	7/23/04 2:00 PM	0.1	2.4	0.22
Water Depth	1.0	18.3	0.459	0.12	7/23/04 5:00 PM	1.01	6.0	0.10
Sediment Depth	0.3	18.1	0.014	0.04	7/23/04 3:00 PM	0.15	2.6	0.20
Sediment Depth	0.7	18.4	0.014	0.04	7/23/04 3:00 PM	0.15	2.6	0.20
Sediment Depth	2	18.6	0.014	0.04	7/23/04 3:00 PM	0.15	2.6	0.2
Bottom width	1	18.5	0.0074	0.0378	7/23/04 2:00 PM	0.15	1.6	0.28
Bottom width	1.5	18.3	0.0106	0.0394	7/23/04 3:00 PM	0.15	2.1	0.24
Bottom width	2.5	18.2	0.0173	0.0411	7/23/04 3:00 PM	0.15	3.1	0.18
Air Temperature	Increase 5°C	18.4	0.014	0.040	7/23/04 3:00PM	0.15	2.6	0.20
Air Temperature	Decrease 5°C	18.1	0.014	0.040	7/23/04 3:00PM	0.15	2.6	0.20
Air Temperature	Increase 10°C	18.6	0.014	0.040	7/23/04 3:00PM	0.15	2.6	0.20

Table 4.3 Sensitivity Coefficients for Baseline 1 Modified Heat Source

Parameter	% Change In Parameter	% Change In The Maximum Seven Day Average of Daily Maximum Temperatures	Sensitivity Coefficient
Air Temperature	25.9	0.84	0.326
	-25.9	-0.84	0.326
	51.75	1.69	0.326
Flow Depth	-33.33	3.80	-0.114
	33.33	-0.93	-0.027
	100.00	-0.54	-0.005
	233.33	0.19	0.008
	566.33	0.61	0.011
	6.67	-0.31	-0.04
	100.00	-0.54	-0.005
	13.33	-0.52	-0.039
Incision	-100.00	-3.86	0.039
	-80.00	-2.91	0.036
	100.00	0.22	0.002
	-10.00	-0.04	0.004
	10.00	0.03	0.003
	-20.00	-0.11	0.005
Side Slope	-50.00	-0.49	0.010
	25.00	0.22	0.009
	50.00	0.76	0.015
Effective Shade From Stream Bank	58.16	-3.86	-0.009
	-33.48	-2.91	-0.023
	-19.05	0.22	-0.011
Effective Shade From Vegetation	343.70	-3.62	-0.011
	233.45	-3.31	-0.014
	-68.20	1.01	-0.015
Bottom Width	-50.00	0.12	-0.002
	-25.00	0.38	-0.015
	25.00	-0.20	-0.008
Sediment Depth	-40.00	-1.43	0.036
	40.00	0.98	0.024
	300.00	2.06	0.007

Flow Depth

Figure 4.5 shows the change in predicted maximum seven day average of daily maximum temperatures versus the change in input depth. As user defined flow depth decreases, the calculated discharge used to model temperature also decreases. The volume of water receiving net-heat exchange is smaller and the system is more dynamic. Maximum Seven Day Average temperature was sensitive to a change in depth, with sensitivity increasing as depth decreases. Increased flow acts to decrease the impact of the heat balance on a reach. If the net flux in a reach is negative, the reach will have less cooling impact on a watercourse with larger flow. If the net flux is positive the watercourse will show less warming if flow is greater. In addition, if increased velocity is the only mechanism increasing flow, a water element will spend less time in the environment and exchange less total energy than an equal, slower moving volume. This is consistent with the relationships and findings of Larson and Larson (1997), Brown (1967) and others. In a channel with sloping sides, the wetted width that can be exposed to solar radiation increases with increasing depth.

Figure 4.5 Sensitivity of the maximum seven day average of daily maximum temperatures to flow depth
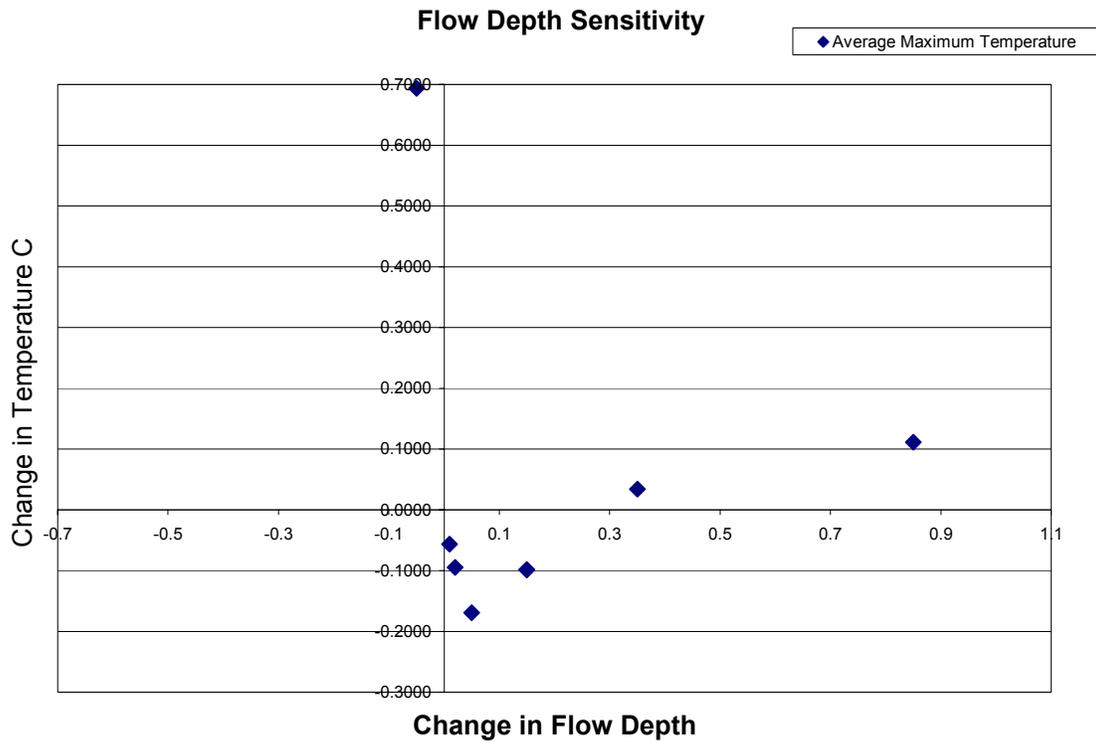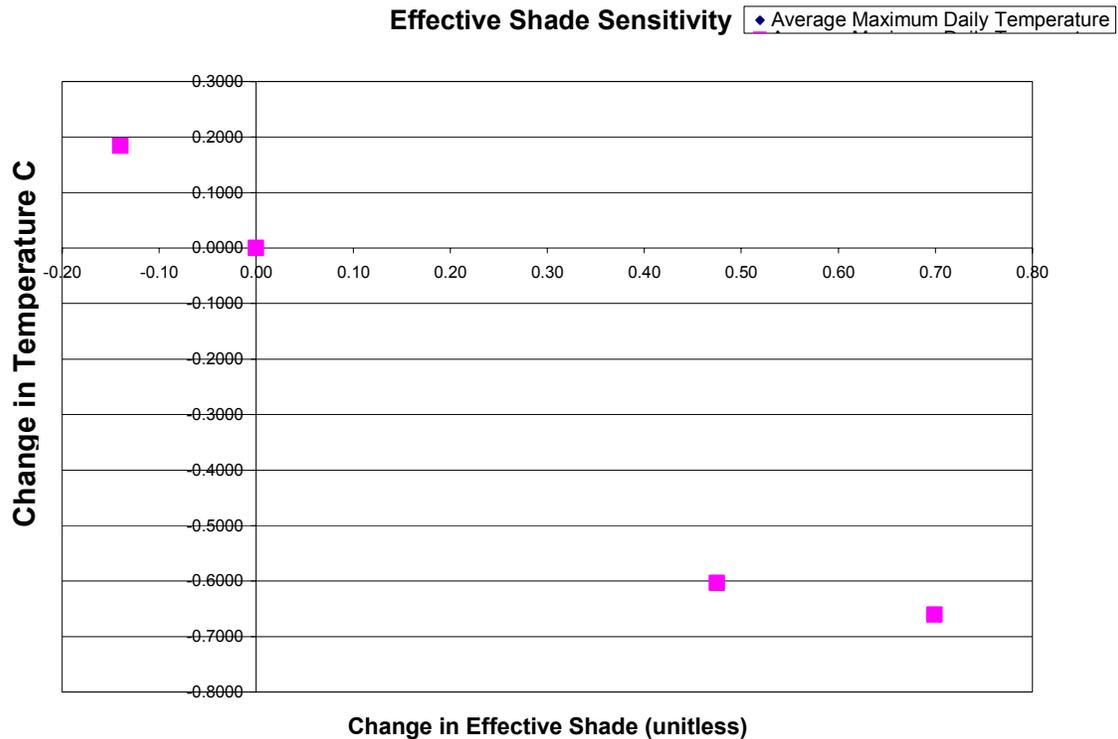

Effective Shade

Figure 4.6 shows the change in the predicted maximum seven day average of daily maximum temperatures versus the change in effective shade. Effective shade is the percent reduction in solar radiation reaching the water's surface. Elements reducing the amount of solar radiation that reaches the water's surface include channel morphology such shade from an incised channel bank, and shade from riparian vegetation. Sensitivity analysis for effective shade was carried out by changing vegetation density, height, width and overhang. The temperature response to change in effective shade is relatively non-linear. The decrease in temperature slows as effective shade increases. This model

behavior is reasonable because as the warming influence of solar radiation is reduced, other warming factors, such as air temperature remain un-changed by shade.

Figure 4.6 Sensitivity of the maximum seven day average of daily maximum temperatures to effective shade

Channel Incision

Figure 4.7 shows the change in predicted maximum seven day average of daily maximum temperatures versus change in channel incision. Channel incision may increase or reduce effective shade depending on channel side slope. For the same incision distance, a bank with a shallower side slope will provide less effective shade. Vegetation at the top of a deeply incised long sloping bank will be farther from the water's surface and must be taller or more overhanging to provide the same shade. Vegetation that takes root between banks is considered either emergent or overhanging. No emergent

76

vegetation is present in this scenario. When channel side slopes are steep, riparian vegetation on the bank remains close to the water's edge, but is effectively taller, casting its shadow a longer distance and providing more effective sky closure of the stream's 180 degree open sky view. The change in temperature with change in incision is also non-linear as is the relationship of temperature to effective shade.

Figure 4.7 Sensitivity of the maximum seven day average of daily maximum temperatures to change in incision depth.
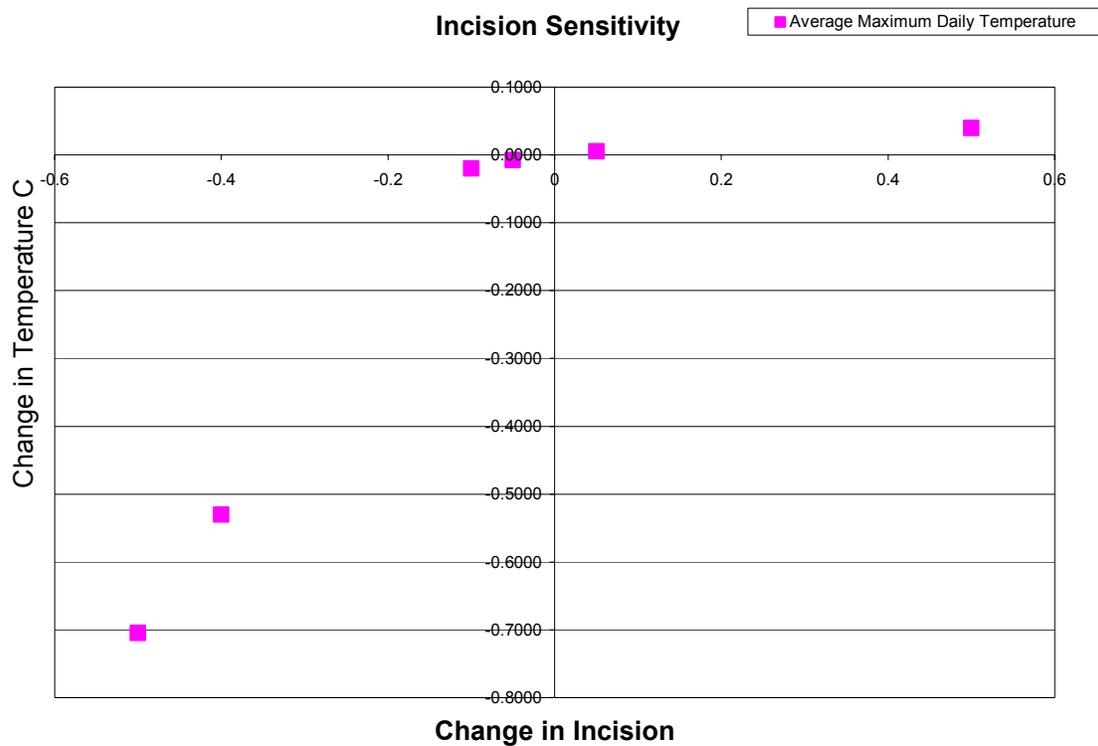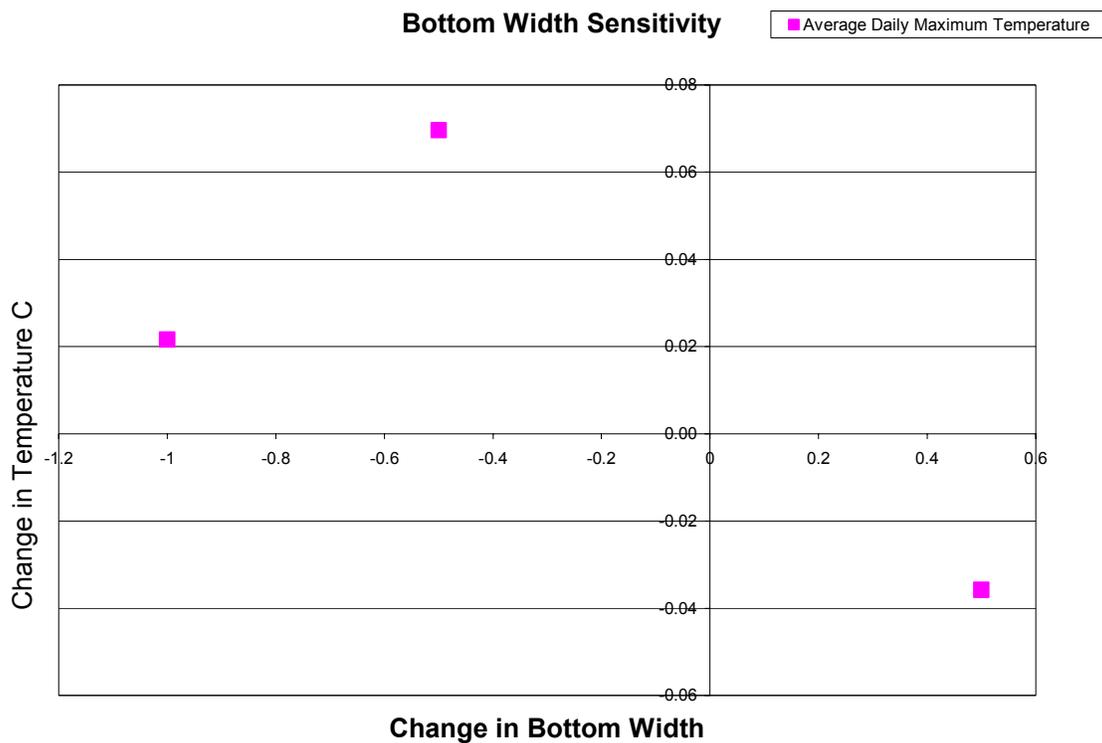

Bottom Width

Figure 4.8 shows the change in predicted maximum seven day average of daily maximum temperatures with change in bottom width. With a fixed water depth, increasing the bottom width has two effects, it increases simulated flow volume by increasing cross-sectional area, and it increases top width and potential surface area

available for energy transfer. In this case, the more significant influence is the increase in flow volume. Under baseline conditions, effective shade is not greatly influenced by the increase in bottom width, so the increase in solar exposure with increased top width is not as important as the increase in volume.

Figure 4.8 Sensitivity of maximum seven day average of daily maximum temperatures to channel bottom width

Bottom width sensitivity simulations represent increasing flow and decreasing effective shade as the bottom width ranges from 1 to 2.5 meters.

Air Temperature

Figure 4.9 shows the change in predicted maximum seven day average of daily maximum temperatures to change in daily air temperatures. Stream temperature shows a relatively linear relationship with air temperature for this baseline scenario over the range

tested. The large slope of the graph of change in water temperature versus change in air temperature indicates high sensitivity. Water temperature has a strong dependence on air temperature for the scenario tested. It is important to remember that the only variable changed in this sensitivity scenario is hourly air temperature. In a realistic scenario, increased air temperatures would also increase the model's upstream temperature boundary condition. This change could result in a greater overall temperature change in response to change in air temperature.

Figure 4.9 Sensitivity of maximum seven day average of daily maximum temperatures to air temperature
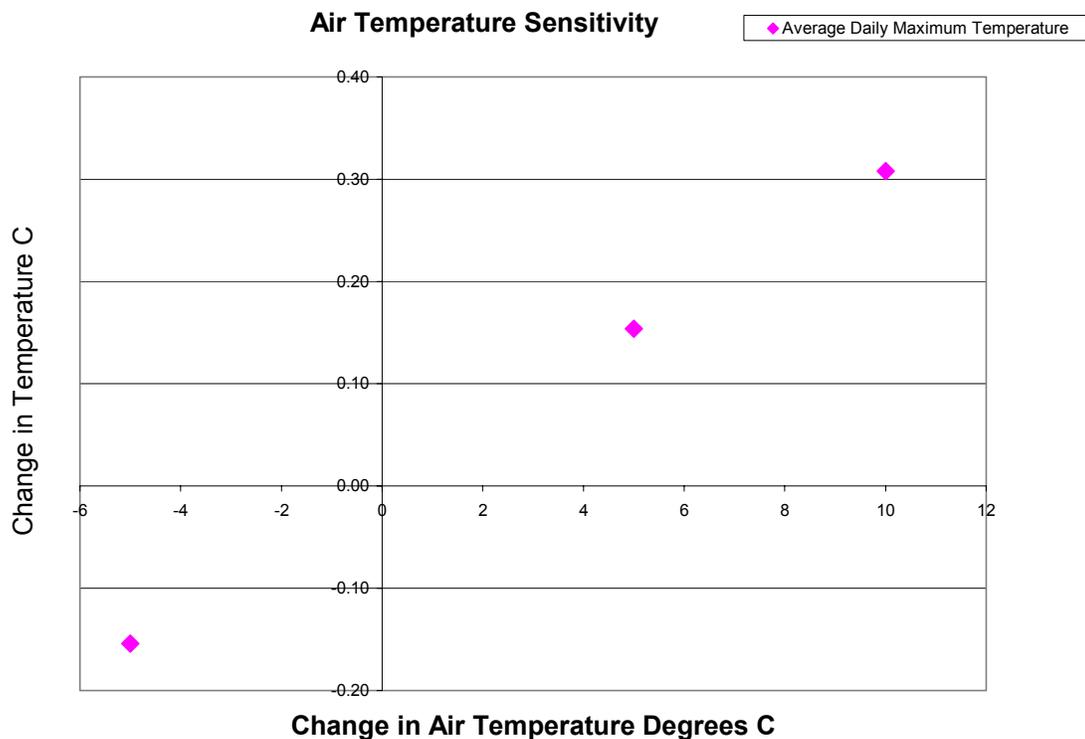
Sediment Depth

Figure 4.10 shows the change in predicted maximum seven day average of daily maximum temperatures with change in channel sediment depth. Recall that the sensitivity coefficient is equal to the percent change in temperature divided by the percent change in input parameter. Results show that decreasing the sediment depth would have a significant impact on temperature prediction, while increasing it significantly has diminishing rate of influence. However, the model assumes that the conducting sediment is similar to soil in density and this may not be thoroughly descriptive of the material that accumulates rapidly on the bottom of slow moving watercourses obstructed by reed canarygrass, which is highly organic and low in density.

Figure 4.10 Sensitivity of seven day average of daily maximum temperatures to sediment depth
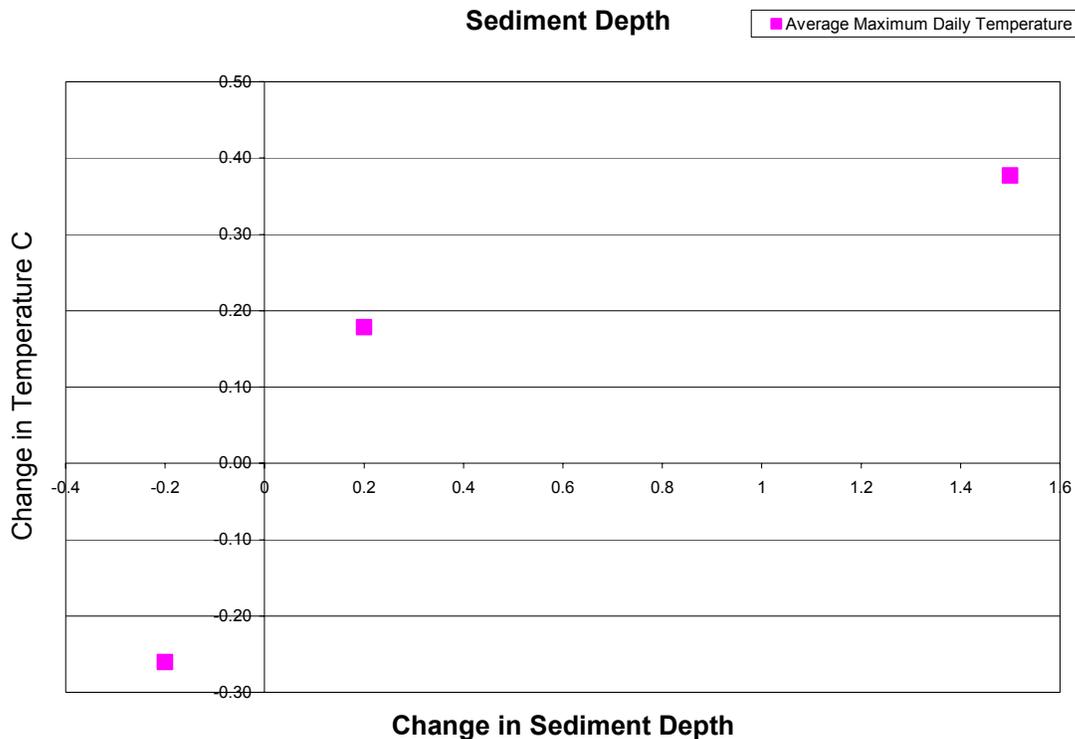
Impact of Channel Morphology on Effective Shade

One difficulty in obtaining representative sensitivity analysis results is that the model's sensitivity to a specific input parameter may change with different values of the same input parameter. Sensitivity also may depend on assumed conditions. For example, the sensitivity of stream temperature to the shade of vegetation may be greater when no bank shade is present. When the bank significantly shades the watercourse, water temperature may not respond to additional shade from vegetation. These assumed conditions, such as stream bank shading, are part of the "baseline" scenario. The baseline scenario is a set of input data used for repeated comparison with simulation results as input values are varied one at a time.

The sensitivity of the system's response to solar radiation and effective shade depends on the channel size and morphology. The second baseline condition used to identify potential sensitivity to effective shade is a channel with vertical side slopes. Consideration of vertical side slopes gives and idea of temperature sensitivities in the extreme case when side slopes are very steep. Input parameters used for baseline 2 are described in the Table 4.4.

Table 4.4 Sensitivity Analysis Input Parameters for Baseline 2 Modified Heat Source

Parameter	Baseline Value	Units
Simulation Period	14	Days
Start date	7/15/04	Date
Lat	42.6	Degrees
Long	-121.6	Degrees
Aspect	180	Degrees
Right Side Slope	0.001	H:V
Left Side Slope	0.001	H:V
Incision	0.5	Meters
Bottom width	1.5	Meters
Water Depth	0.15	Meters
Manning's n	0.2	
Channel gradient	0.001	
Right Bank Vegetation	RCG	
Left Bank Vegetation	RCG	
Sediment Depth	0.5	Meters
Sediment Temperature	13.7	Degrees C

Table 4.5 shows the detailed results for sensitivity analysis using baseline scenario 2. As each parameter is varied in sensitivity analysis using baseline 2, it influences the value of other parameters. Consideration of the values of other parameters as presented in table 4.5, aids in analysis and explanation of sensitivity analysis results.

Table 4.5 Sensitivity Analysis Results for Baseline Scenario 2

Test Parameter	Test Parameter Value	Maximum 7-Day Average of Daily Maximum Temperature °C	Discharge	Flow Velocity	Date and Time of Maximum	Depth	Wetted Width	Effective Shade
Baseline		17.9	0.009	0.04	7/23/04 5:00 PM	0.15	1.5	0.80
Air Temperature	Increase 5°C	18.1	0.009	0.04	7/23/04 5:00 PM	0.15	1.5	0.80
Air Temperature	Decrease 5°C	17.8	0.009	0.04	7/23/04 5:00 PM	0.15	1.5	0.80
Air Temperature	Increase 10°C	18.2	0.009	0.04	7/23/04 5:00 PM	0.15	1.5	0.80
Flow Depth	0.3	18.2	0.03	0.06	7/23/04 5:00 PM	0.3	1.5	0.80
Flow Depth	0.25	18.2	0.02	0.05	7/23/04 5:00 PM	0.25	1.5	0.80
Flow Depth	0.13	17.9	0.01	0.04	7/23/04 3:00 PM	0.13	1.5	0.80
Flow Depth	0.1	17.9	0.01	0.03	7/23/04 3:00 PM	0.1	1.5	0.80
Bank Incision	0.1	17.9	0.008	0.04	7/23/04 4:00 PM	0.15	1.5	0.76
Bank Incision	1.0	17.9	0.008	0.04	7/23/04 4:00 PM	0.15	1.5	0.83
Bank Incision	0.7	17.9	0.008	0.04	7/23/04 4:00 PM	0.15	1.5	0.82
No Vegetation	0.21	18.4	0.008	0.04	7/23/04 4:00 PM	0.15	1.5	0.21
Willows	0.99	17.5	0.008	0.04	7/23/04 5:00 PM	0.15	1.5	0.99
Willows (50%)	0.84	17.6	0.008	0.04	7/23/04 5:00 PM	0.15	1.5	0.84
Bottom Width	0.5	17.4	0.002	0.033	7/23/04 6:00 PM	0.15	1.5	0.96
Bottom Width	0.2	18.0	0.012	0.041	7/23/04 5:00 PM	0.15	1.5	0.76
Bottom Width	1.0	17.9	0.005	0.037	7/23/04 5:00 PM	0.15	1.5	0.87
Sediment Depth	0.7	18.1	0.008	0.04	7/23/04 5:00 PM	0.15	1.5	0.80
Sediment Depth	0.3	17.7	0.008	0.04	7/23/04 5:00 PM	0.15	1.5	0.80
Sediment Depth	2.5	17.5	0.008	0.04	7/23/04 5:00 PM	0.15	1.5	0.80

Table 4.6 Sensitivity Coefficients for Baseline 2 Sensitivity Analysis Results Modified Heat Source

Parameter	% Change In Parameter	% Change In The Maximum Seven Day Average of Daily Maximum Temperatures	Sensitivity Coefficient
Air Temperature	25.87	0.71	0.027
	-25.87	-0.70	0.027
	51.75	1.42	0.027
Flow Depth	66.67	0.87	0.013
	-13.33	-0.31	0.023
	-33.33	-0.48	0.014
Incision	-80.00	0.00	0.000
	100.00	0.00	0.000
	40.00	0.00	0.000
Effective Shade From Vegetation	-73.41	2.25	-0.031
	24.63	-2.39	-0.100
	5.36	-2.28	-0.430
Bottom Width	-66.67	-3.23	0.049
	33.33	0.04	0.001
	-33.33	-0.08	0.003
Sediment Depth	40.00	0.80	0.012
	-40.00	-1.74	0.044
	-50.00	-2.56	0.051

Table 4.6 presents sensitivity analysis results for baseline scenario 2. The sensitivity of this baseline scenario to air temperature shade is much smaller than the sensitivity of baseline 1 to air temperature, while the sensitivity of effective shade is greater.

Effective Shade From Vegetation

Sensitivity results obtained using baseline 2 are outlined in table 4.5. Effective shade was tested by changing the density and type of vegetation in the same way as in baseline 1 sensitivity analysis, however the percent change in effective shade that results

is generally smaller. One reason for this difference is that baseline 2 has a higher starting effective shade than baseline 1, so the percent change in effective shade due to increasing vegetation density is smaller. The temperature response to increased effective shade remains significant within the range tested. As a result the sensitivity coefficient for effective shade indicates high sensitivity. One reason that the temperature response remains significant is the smaller volume of water contained within the banks has a larger temperature response to energy input than the larger volume in baseline 1. The sensitivity of baseline 2 to effective shade is relatively non-linear. The greatest sensitivity occurs with a small increase in effective shade. This result is consistent with the results in baseline 1, where decreasing sensitivity with increasing effective shade was observed. Temperature decreases only slightly more with continued increase in effective shade.

Air Temperature and Sediment Sensitivity

As in the first baseline scenario, the sensitivity of this baseline to air temperature is relatively linear. Again in this scenario, the only variable altered was hourly air temperature. The upstream boundary water temperature did not change, as it would have in a realistic scenario. The sensitivity coefficient is smaller, indicating that a watercourse with characteristics described by baseline 2 is not as sensitive to air temperature as the one described by baseline 1. One reason for this decreased sensitivity is that less water surface area is in contact with air than would be for a wider channel. The sensitivity of this baseline to sediment temperature is slightly less sensitive for a similar reason. The channel is not as wide, and conduction is assumed to occur only along the channel bottom. With a narrower channel less water is in contact with the conducting sediment.

Incision Depth

For this baseline scenario, there was no nearly no temperature response to a change in bank incision. The reason for this may be the presence of dense vegetation at the water's edge as defined by the baseline conditions. With nearly vertical banks, reed canarygrass exists on the banks at the water's edge. Reed canarygrass is more than a meter tall and simulated at 93% density so it casts shadows similar to the shadow from an opaque bank.

Sensitivity Analysis Discussion

It is important to realize that a single sensitivity of predicted temperature to effective shade does not indicate the magnitude of temperature change, it indicates the ratio of change in temperature to change in parameter. Because many sensitivities are non-linear, a high sensitivity to an input parameter around one range of values does not necessarily suggest that temperature will have the same relationship to the parameter around other values. The greatest change in temperature for the baseline 2 sensitivity scenarios, occurred with a 66% reduction in bottom width but the sensitivity coefficient was not the highest because the large change in bottom width required to obtain this decrease in temperature.

Management Scenarios

To compare the thermal impact of potential management scenarios, different channel morphologies and riparian vegetation types are used to simulate temperature with the constraint of constant discharge. The baseline scenario used to evaluate management scenarios represents a watercourse designed to be 2 meters in width, with 2:1 side slopes. Channel discharge is approximately 0.5 cfs for all management scenarios. Reed canarygrass vegetation is assumed to occupy the bank and not obstruct or shade the middle of the watercourse. Based on field observations and maintenance plans, these are reasonable parameters for a watercourse that has been recently maintained but has not received riparian plantings. Under real field conditions, maintenance activities have been observed to increase groundwater flow and occasionally to access groundwater springs that feed additional cool flow into a channel. While this is a possibility particularly in wet years, the amount of ground water supplied to a channel and the increase in groundwater due to maintenance will be irregular. The cooling impact due to a possible increase in groundwater flow with maintenance should not be considered in the analysis of the impact of maintenance on channel design. Neglecting groundwater flow provides a reasonable worst case scenario and highlights the influence of maintenance design parameters.

Table 4.7 outlines maintenance scenarios considered. Maintenance scenarios are considered in comparison with a baseline condition to determine the relative impact of design options. The predicted Maximum Seven-Day Average of Daily Maximum Temperatures is 18.3°C under the baseline condition. Simulation takes place in mid-July

using weather data for King County during July 2004. Temperatures in the region during July 2004 were considered "Much Above Normal" by the National Oceanic and Atmospheric Administration (http://www.ncdc.noaa.gov/oa/climate/research/2004/jul/currentmonth.html#trD_mo).

Table 4.7 Management Scenario Results

	Side Slopes	Vegetation	Bottom Width (Meters)	Flow Velocity (Meters/sec)	Flow Depth (Meters)	Effective Shade (0-1)	Max 7-Day Average of Daily Maximum Temperature
Baseline	2:1	RCG	2	0.04	0.15	0.20	18.3
Scenario 1	0:1	RCG	1	0.05	0.28	0.87	18.2
Scenario 2	2:1	None	2	0.04	0.15	0.06	18.4
Scenario 3	0:1	None	1	0.05	0.28	0.31	18.2
Scenario 4	2:1	Willows	2	0.04	0.15	0.90	17.6
Scenario 5	0:1	Willows	1	0.05	0.28	0.99	18.0

Management Scenario 1

Refer to Table 4.7 for a summary of the conditions and results of this management scenario. Recall that for this maintenance scenario, water discharge was held constant with that of the baseline 1 simulation with a smaller bottom width, deeper water column, and steeper 0.001:1 side slope. Simulated Maximum Seven Day Average of Daily Maximum Temperatures was 18.2°C. With narrower and deeper flow dimensions the predicted Maximum Seven Day Average Temperature showed a 0.1°C decrease. This decrease in temperature indicates a cooling trend over the reach. Because the flow velocity is slightly higher than that of the baseline, water moving through this system is not exposed to the surroundings as long as it is in the baseline scenario. This gives the environmental thermal balance less influence on water temperature.

Management Scenario 2

Refer to Table 4.7 for a summary of the conditions and results of this management scenario. The same input parameters were used as in the listed baseline simulation, however all vegetation is assumed to be cleared. Conditions used in this scenario are similar to conditions following watercourse maintenance and before mitigation plantings. The predicted Maximum Seven Day Average Temperature increased 0.1°C under these conditions. This indicates a warmer trend over the reach in comparison with the baseline. The velocity of flow and exposure time within this system is the same as that of the baseline, so the influence of the environmental energy balance on has the same potential influence on watercourse temperature as it does in the baseline.

Management Scenario 3

Refer to Table 4.7 for a summary of the conditions and results of this management scenario. In comparison with Management Scenario 2, this scenario represents the deeper narrower and quicker moving flow. Flow velocity is the same in this scenario as in Scenario 1, however, no vegetation is assumed to exist on the banks or in the channel. With no vegetation, the narrower channel shows a predicted Average Daily Maximum Temperature that is cooler than the baseline predicted Average Daily Maximum Temperature. The increase in effective shade in comparison with the baseline scenario is due to bank incision and a narrower water width. This scenario represents conditions similar to a watercourse with steep banks following watercourse maintenance.

Management Scenario 4

Refer to Table 4.7 for a summary of the conditions and results of this management scenario. This scenario considers the wider, shallower, and slower moving watercourse simulated in Scenario 1, Willow trees were simulated on the banks. The highest effective shade considered so far, due primarily to willow trees, combined with the slowest time of travel through the system result in the largest water temperature impact and the most cooling. The Maximum Seven Day Average of Daily Maximum Temperatures predicted in Scenario 4 is 0.7 degrees C cooler than the baseline Scenario. This condition is similar to a watercourse with shallow banks planted with willow vegetation more than two years after maintenance and successful mitigation planting of willows.

Management Scenario 5

Refer to Table 4.7 for a summary of the conditions and results of this management scenario. Management Scenario 5 is the most similar to Scenario 1 and with similar temperature prediction results. Applying willow vegetation to the banks of the narrower, deeper, quicker moving watercourse increases effective shade slightly. With the shorter travel time, this is enough to reduce the predicted Maximum Seven Day Average of Daily Maximum Temperatures only 0.1 degrees C.

Chapter 5

SUMMARY

The goal of this study was to identify the reach scale change in temperature associated with watercourse maintenance and to produce a modeling tool to predict watercourse temperature under different management scenarios. A modified temperature model was developed capable of simulating pre-and post maintenance conditions. These conditions include wetland flow and extensively emergent or overhanging vegetation present before maintenance as well as changes in channel morphology and vegetation due to excavation. Results show that the developed model can reasonably predict diurnal and maximum seven day average of daily maximum temperatures. Hourly temperature predictions are typically accurate to within less than half a degree. Simulation results can be used to compare downstream watercourse temperature before and after planned maintenance, or to generate predicted temperature data for use in modeling dissolved oxygen. Predicted Maximum Seven Day Average of Maximum Daily Temperatures can be used to determine habitat suitability and determine compliance with temperature standards according to EPA's temperature standard guidance before and after planned maintenance.

The modified model can be used to simulate maintenance and mitigation scenarios in order to identify the impact of planned maintenance or to select mitigation and maintenance with the minimum impact. As part of this objective, the model can be used to identify the potential importance and effectiveness of riparian vegetation in

protecting watercourse temperature from increase due to maintenance. Sensitivity

analysis results and management scenarios show low sensitivity and small temperature

response to reach conditions. The small changes observable due to changes within a reach

suggest that the upstream temperature boundary condition is a strong controlling factor.

Considering the small temperature changes that are observable, sensitivity analysis

results show that a steep incised bank increases the effectiveness of vegetation in

providing riparian shade, and that shade cast by vegetation and the bank itself can

decrease maximum seven day average temperatures by at least 0.7 °C. Several studies

site temperature changes of several degrees as a result of changes to riparian vegetation

(Brown 1967, Chen 1997, Doug 1998, Bartholow 2000). It is important to consider that

greater temperature change that those found in this study may be observed for longer

reaches.

Sensitivity scenarios and management scenario results show that shade can play a

role in determining the stream energy balance and temperature; however the maximum

observed change in temperature was 0.7 °C, while model error was approximately 0.5 °C.

The small temperature response indicates the relatively small influence that conditions in

a short reach can have on watercourse temperature. Riparian vegetation can have the

greatest influence on watercourse temperature for watercourses with vertical side slopes,

since vegetation is closest to the water's edge. Emergent vegetation may provide

significant shade, but it obstructs drainage. Willows with significant overhang provide an

adequate shade to mitigate for the removal of emergent reed canarygrass during

maintenance. Sitka willows, Himalayan Blackberry and reed canarygrass were found to

be similar in calibrated shade density, ranging from 80% to 100%. The dimensions of Sitka willow after its second year of successful growth make it the most effective in providing short-term shade. The calibrated density for mature willows was approximately 93%. This calibrated density accurately simulated solar radiation in the shade of willows spaced one to four feet apart at their base. A shade calibration was not made for willow stakes in the first summer following fall planting, because no effective shade could be measured. Willows growing successfully more than two years old and planted on one foot spacing were found to have a calibrated density of 80%. Because calibrated vegetation densities did not vary widely among the types of vegetation used in this study, the most important factor determining the effectiveness of vegetation in providing watercourse shade is the amount of shade coverage, and not shade density. The greatest coverage is made possible by tall vegetation with long overhang lengths planted close to the water's edge, such as willows. Of the three vegetation types studied, willows have the greatest potential for providing overhang. If willows trees are grown successfully, willows planted on one bank may be sufficient to shade watercourses of typical size after two successful growing seasons. The model should be applied on a case by case basis to determine the temperature benefit of riparian plantings for a particular watercourse and maintained channel morphology. The absolute change in temperature observed along the length of a reach will depend on reach length, the upstream temperature entering the reach, the time of travel, and the thermal environment within the reach. Each of these factors is considered in the modified model.

Without accurate flow measurements, and information about groundwater exchange, neither field observed nor simulated changes in actual temperature can be attributed to the presence or absence of shade from vegetation. Modeling scenarios neglecting ground water flow can provide an indication of the *potential* influence of remaining factors. Because the inflow of ground water will vary by year and location, it should not be considered in scenarios used to plan watercourse mitigation. Ground water will generally have a cooling effect, and neglecting this effect provides a reasonable worst case scenario that was likely attained during the validation period in the warm drought years during which validation data was collected. A single statement regarding the importance of shade versus ambient temperature cannot be made for all small agricultural drainage watercourses in King County. The influence and relative importance of various factors will depend on channel morphology at a minimum. Air temperature may be more important in determining the temperature of wide watercourses with sloped banks, while shading vegetation may play a more important role than air temperature for narrower watercourses with vertical banks.

BIBLIOGRAPHY

Beschta, R. L and J. Weatherred. 1984. A computer model for predicting stream temperatures resulting from the management of streamside vegetation. USDA Forest Service. WSDG-AD-00009.

Bartholow, John M. 2000 The Stream Segment and Stream network Temperature Models: A Self-Study Course. Version 2.0, USGS Biological Resource Division Midcontinent Ecological Science Center, Fort Collins Colorado.

Barthoolow, John M. 2000 Estimating cumulative effects of clearcutting on stream temperatures, Rivers, 7(4) , 284-297

Bormann, M. 2000. The grazier, Oregon State University Extension Service. Vol. 306 no.5

Boyd, M. S. 1996. Heat Source: stream temperature prediction. Master's Thesis. Departments of Civil and Bioresource Engineering. Oregon State University, Corvallis, Oregon.

Boyd, M. S. and Kasper, B. 2004. Analytical Methods for Dynamic Open Channel Heat and Mass Transfer: Methodology for the Heat Source Model Version 7.0.

Brady, D.K., W. L. Graves, and J. C. Geyer. 1969. Surface heat exchange at power plant cooling lakes, Report 5, Johns Hopkins University Press, Baltimore, MD.

Brown, G. W. 1969, Predicting temperatures of small streams. *Water Resour. Res*. 5(1): 68-75

Brown, G. W. and J. T. Krygier. 1970. Predicting the effects of clearcutting on stream temperature. *Journal of Soil and Water Conservation*. 25: 11-13

Brown, L.C. and Barnwell, T.O., 1987. The Enhanced Stream Water Quality Models QUAL2E and QUAL2E-UNCAS: Documentation and User Manual. EPA/600/3-87/007, Athens, GA.

Chen, Y.D. 1996. Hydrologic and Water Quality Modeling for Aquatic Ecosystem Protection and Restoration in Forest Watersheds: A Case Study of Stream Tmeperature in the Upper Grande Rhonde River, Oregon. Ph.D. dissertation, University of Georgia, Athesn, GA 268 pp.

Chen,Y.D., S.C. McCutcheon, R.F. Carsel, D.J. Norton, J.P. Craig 1997. Enhancement and Application of HSPF for Stream Temperature Simulation in Upper Grande Ronde Watershed, Oregon.

Chen, D.Y., Carsel, R.F., McCutcheon,S.C. and Nutter.W.L. 1998. Stream Temperature Simulation Of Forested Riparian Areas: I Watershed-Scale Model Development. Journal of Environmental Engineering. Vol 124, No.4.

Crites, R. and Tchobanoglous, G. 1998. Small and Decentralized Wastewater Management Systems.McGraw-Hill, New York.

Doug, J., Chen, J., Brosofske, K. D., and R. J. Naiman. 1998. Modeling air temperature gradients across managed small streams in Western Washington. Journa of Environmental Management. 53, 309-321.

Edinger, J. E., Duttweiler, D.W., JGeyer, J.C. 1968. The Response of WaterTemperatures to Meteorological Conditions. *Water Resources Research*. vol. 4 no. 5.

Larson and Larson 1996 . Riparian Shade and Stream Temperature: A Perspective. *Rangelands*. vol 18. no. 4

Larson, A., Larson, P. 1997. The Natural Heating and Cooling of Water. *Rangelands*. vol. 19 no.6.

Larson, A., Larson, P. 2003. The Rebuttal: Perspectives on water flow and interpretations of FLIR images". *Range Journal of Range Management*. vol. 55 pg 106-111.

Sullivan et al. 1990 Evaluation of prediction models and characterization of stream temperatureregimes in Washington Timber/Fish/Wildlife Rep No

Ibqal, M. 1983. An Introduction to Solar Radiation. Academic Press. New York. 213 pp.

McCutcheon, S.C., and Martin, J. L., 1999. Hydrodynamics and Transport for Water Quality Modeling. CRC Press, Boca Raton, Florida.

Meehan, W. R., editor. 1991. Influences of forest and rangeland management on salmonid fishes and their habitats. American Fisheries Society Special Publication 19.

Moore, J.,Miner, J. and Bower, R. 1999. The Effect of Shade on Water: A Tub Study. Department of Bioresource Engineering. Oregon State University.

NOAA Fisheries. 2004. Consultation on Remand for Operation of the Columbia River Power System and 19 Bureau of Reclamation Projects in the Columbia Basin. F/NWR/2004/00727

Petersen, B.T. Stringham and W. Krueger. 1999. The impact of shade on the temperature of running wataer. Department of Rangeland Resources. Oregon State University.

Shannon &Wilson, Inc. 2002. Mullen Slough Subbasin Habitat Limiting Factors Report. Shannon & Wilson, Inc. Geotechnical and Environmental Consultants.

Theurer, F. D., K. A. Voos, and W. J. Miller. 1984. Instream Water Temperaturea Model. Instream Flow Inf. Pap. 16. U. S. Fishe and Wildl. Serv. FWS/OBS-84-15. v.p.

Wunderlich. 1972. Heat and mass transfer between a water surface and the atmosphere. Tennesee Valley Authority. Water Resources Research Laboratory Report no 14. Norris, Tennessee. p. 420

U.S. Army Corps of Engineers, Seattle District (USCOE). 1997. "Mill Creek Basin, King County, Washington Aquatic Resources Restoration Plan.

US Environmental Protection Agency. 2003. EPA *Region 10 Guidance for Pacific Northwest State and Tribal Temperature Water Quality Standards*. EPA 910-B-03-002. Region 10 Office of Water, Seattle, WA

Zwieniecki, M.A., and M. Newton. 1999. Influence of streamside cover and stream features on temperature trends in forested streams of western Oregon. Western Journal of Applied Forestry vol.14. no.2, 106-113